The emergence of successful *Streptococcus pyogenes* lineages through convergent pathways of capsule loss and recombination directing high toxin expression

Claire E. Turner[1,2#], Matthew T. G. Holden[3,4], Beth Blane[5], Carolyne Horner[6], Sharon J. Peacock[5], Shiranee Sriskandan[2].

[1]Molecular Biology & Biotechnology, The Florey Institute, University of Sheffield

[2]Department of Infectious Diseases, Imperial College London

[3]Pathogen Genomics, The Wellcome Trust Sanger Institute, Cambridge, United Kingdom

[4] School of Medicine, University of St Andrews, St Andrews, United Kingdom

[5] Department of Medicine, University of Cambridge, Cambridge, United Kingdom

[6] British Society for Antimicrobial Chemotherapy, Birmingham, United Kingdom

Corresponding author:

Dr Claire Turner

Molecular Biology & Biotechnology

Firth Court

Western Bank

Sheffield

UK

S10 2TN

c.e.turner@sheffield.ac.uk

Abstract

Gene transfer and homologous recombination in *Streptococcus pyogenes* has the potential to trigger the emergence of pandemic lineages, as exemplified by lineages of *emm*1 and *emm*89 that emerged in the 1980s and 2000s respectively. Although near-identical replacement gene transfer events in the *nga* (NADase) and *slo* (Streptolysin O) locus conferring high expression of these toxins underpinned the success of these lineages, extension to other *emm*-genotype lineages is unreported. The emergent *emm*89 lineage was characterised by five regions of homologous recombination additional to *nga/slo*, including complete loss of the hyaluronic acid capsule synthesis locus *hasABC*, a genetic trait replicated in two other leading *emm* types and recapitulated by other *emm* types by inactivating mutations. We hypothesised that other leading genotypes may have undergone a similar recombination events. We analysed a longitudinal dataset of genomes from 344 clinical invasive disease isolates representative of locations across England, dating from 2001 to 2011, and an international collection of *S. pyogenes* genomes representing 54 different genotypes, and found frequent evidence of recombination events at the *nga-slo* locus predicted to confer higher toxin expression. We identified multiple associations between recombination at this locus and inactivating mutations within *hasA/B*, suggesting convergent evolutionary pathways in successful genotypes. This included common genotypes *emm*28 and *emm*87. The combination of no or low capsule, and high expression of *nga* and *slo*, may underpin the success for many emergent *S. pyogenes* lineages of different genotypes, triggering new pandemics and could change the way *S. pyogenes* causes disease.

48 **Importance**

49 *Streptococcus pyogenes* is a genetically diverse pathogen, with over 200 different genotypes
50 defined by *emm* typing, but only a minority of these genotypes are responsible for majority of
51 human infection in high income countries. Two prevalent genotypes associated with disease
52 rose to international dominance following recombination of a toxin locus that conferred
53 increased expression. Here, we found that recombination of this locus and promoter has
54 occurred in other diverse genotypes, events that may allow these genotypes to expand in the
55 population. We identified an association between the loss of hyaluronic acid capsule
56 synthesis and high toxin expression, which we propose may be associated with an adaptive
57 advantage. As *S. pyogenes* pathogenesis depends both on capsule and toxin production, new
58 variants with altered expression may result in abrupt changes in the molecular epidemiology
59 of this pathogen in the human population over time.

60

Introduction

The capacity for the bacterial human pathogen *Streptococcus pyogenes* to undergo genetic exchange, independent of known bacteriophages or mobile elements, is not well understood, yet recent evidence suggests it underpins the emergence of successful new variants that rapidly rise to international dominance. Homologous recombination of a chromosomal region encompassing the toxin genes *nga* (encoding for NADase), *ifs* (encoding the inhibitor for NADase) and *slo* (encoding for Streptolysin O), which was dated to have occurred in the mid-1980s, is thought to have driven the rise of *emm*1 to almost global dominance (1). The homologous recombination event resulted in increased *nga*/*slo* expression compared to the previous variant, linked to the gain of a highly active *nga/ifs/slo* promoter in the new *emm*1 variant compared to the previous variant (2).

A very similar recombination event was recently identified in the genotype *emm*89. A new variant of *emm*89 sequence type (ST) 101 (also referred to as Clade 3) emerged, having undergone six regions of predicted homologous recombination compared to its ST101 predecessor (also referred to as Clade 2) (3, 4). One of the six regions encompassed the *nga/ifs/slo* locus, comprising a region almost identical to *emm*1, that conferred similarly high expression of *nga* and *slo* compared to the previous variant. Another recombination region within the emergent ST101 *emm*89 resulted in the loss of the hyaluronic acid capsule. We dated the emergence of this new acapsular, high toxin expressing ST101 *emm*89 lineage to the mid-1990s, but there was a rapid increase and rise to dominance in the UK between 2005-2010 (3). The lineage is now the dominant form of *emm*89 in the UK as well as other parts of the world including Europe, North America and Japan (4-8).

Given that recombination associated with *nga*/*ifs*/*slo* can give rise to new successful *S. pyogenes* variants, we hypothesised that this may be a feature common to other successful

emm-types. To determine if this is the case, we sequenced the genomes of 344 *S. pyogenes* invasive disease isolates originating from hospitals across England between 2001-2011, and compared the data with other available historical and contemporary international *S. pyogenes* whole genome sequence (WGS) data. We identified that recombination of the *nga-ifs-slo* locus has occurred in other leading *emm*-types, supporting the hypothesis that it can underpin the emergence and success of new lineages. We also identified an association of *nga-ifs-slo* recombination towards a high activity promoter variant with inactivating mutations within the capsule locus. This suggests that loss of capsule may also provide an advantage to certain genotypes, either through a direct effect on pathogenesis or an association with the process of recombination.

Results

Genetic characterisation of bacteraemia isolates

We performed whole genome sequencing of 344 *S. pyogenes* invasive isolates collected from hospitals across England by the British Society for Antimicrobial Chemotherapy (BSAC) Bacteraemia Resistance Surveillance Programme during 2001-2011. Forty-four different *emm*-types were identified from *de novo* assembly, with the most common being *emm*1 (n=64, 18.6%), *emm*12 (n=34, 9.9%), *emm*89 (n=32, 9.3%), *emm*3 (n=28, 8.1%), *emm*87 (n= 22, 6.4%) and *emm*28 (n=15, 4.4%) (Supplementary Figure 1). Antimicrobial susceptibilities were typical for *S. pyogenes* with 100% isolates susceptible to penicillin, and 20% resistant to macrolides; detailed susceptibilities and associated genotypes are reported in Supplementary Table 1.

The phylogenetic distribution of the 344 isolates based on core genome variation revealed distinct clustering by *emm*-type, each forming single lineages with the exceptions of *emm*44,

*emm*90 and *emm*101, each of which formed two lineages (Figure 1A). Pairwise distances between isolates gave a median of just 45 SNPs separating the genomes of isolates of the same *emm*-genotype (range 0-15,137 SNPs), compared to a median of 15,648 SNPs separating the genomes of isolates of different *emm*-types (range 5312-18,317 SNPs) (Figure 1B). The genotypes *emm*44, *emm*90 and *emm*101 gave the highest SNP distance for the intra-*emm* comparison (13,494 - 15,137 SNPs) which approaches the median level observed between *emm*-types. This indicated that while other genotypes represent a relatively conserved chromosomal genetic background, the populations of *emm*44, *emm*90 and *emm*101 exhibit more diverse chromosomal backgrounds despite representing the same *emm*-type, potentially due to *emm* gene switching.

High level of variation within the nga-ifs-slo *locus*

In order to identify the level of variation within the *nga-ifs-slo* locus we extracted the sequence from the 3' end of *nusG* (immediately upstream of *nga*) to the 3' end of *slo* (P-*nga-ifs-slo*), comprising the entire locus and all upstream sequence including the predicted ~67bp *nga/ifs/slo* promoter region (9). We constructed a phylogenetic tree from SNPs within P-*nga-ifs-slo* region and compared it to the phylogeny constructed with SNPs extracted from a whole genome comparison to a reference *emm*89 genome, H293 (Figure 2). In most cases, a single unique P-*nga-ifs-slo* variant was associated with each *emm* genotype, consistent with a conserved chromosome. The main exception to this was the P-*nga-ifs-slo* variant found in modern (post 1980s M1T1) *emm*1, which was also found in all *emm*12, all *emm*22 (a lineage known to be acapsular), and 11 of the 32 *emm*89 isolates. These 11 *emm*89 represented the emergent acapsular ST101 variant, whilst the remaining 21 *emm*89 isolates represented the original encapsulated ST101 variant, with a different unique P-*nga-ifs-slo* as previously reported (3). The entire *emm*75 population and one of the two *emm*76 isolates were associated with a P-*nga-ifs-slo* variant that was closely related to the *emm*1-like variant. All

but two *emm*87 isolates had a P-*nga-ifs-slo* variant also found in the acapsular lineage *emm*4 (Figure 2). The presence of multiple P-*nga-ifs-slo* variants within single *emm* genotypes, where the core chromosome was otherwise relatively conserved, indicated that gene transfer and recombination are responsible for the variation rather than extensive genome-wide divergence or *emm* 'switching'.

Variants of the nga-ifs-slo *promoter associated with altered expression*

Recombination of P-*nga-ifs-slo* and surrounding regions in *emm*1 and *emm*89 conferred higher activity and expression of NGA and SLO (1, 3, 10). This change in expression was linked to the combination of three key residues at -27, -22 and -18 within the *nga-ifs-slo* promoter. $A_{-27}G_{-22}T_{-18}$ at these key sites was associated with high *nga-ifs-slo* promoter activity in *emm*1 and emergent *emm*89 following recombination (also referred to as Pnga3) compared to low promoter activity of historical *emm*1 and *emm*89, associated with the key site combinations $A_{-27}T_{-22}C_{-18}$ and $G_{-27}T_{-22}T_{-18}$ respectively (2) (Figure 3A). We compared the ~67bp *nga-ifs-slo* promoter region of the 344 BSAC collection isolate genomes to identify different variants. We expanded the data analysed by including assembled genome data from over 5000 isolates representing 54 different *emm* types: from Cambridge University Hospital (CUH) (11), the rest of England and Wales collected by Public Health England (PHE) in 2014/2015 (PHE-2014/15) (12, 13) and from the USA collected by the Active Bacterial Core Surveillance System (ABCs) in 2015 (ABCs-2015) (14). We excluded 39 *emm*-types represented by fewer than 3 isolates (Supplementary Table 2).

Four combinations of the -27, -22 and -18 residues were found across all 5271 isolates (Table 1); variant 1 $A_{-27}T_{-22}C_{-18}$ and variant 2 $G_{-27}T_{-22}T_{-18}$ are associated with low promoter activity, while variant 3 $A_{-27}G_{-22}T_{-18}$ and variant 4 $A_{-27}T_{-22}T_{-18}$ are associated with high promoter

158 activity. We also identified subtypes of the 67bp promoter region which varied at bases other
159 than -27, -22 and -18 (Figure 3A and B, Table 1). $A_{-27}T_{-22}C_{-18}$ variant subtype 1.1 and $G_{-27}T_{-22}T_{-18}$ variant subtype 2.1 have both previously been confirmed to have low promoter activity
161 (2) and were the most common variants found across genotypes. Other subtypes of these
162 variants were restricted to single genotypes except $G_{-27}T_{-22}T_{-18}$ variant subtype 2.2, which
163 differed by a single substitution of C for a T residue at -40bp. Two subtypes of the high
164 activity variant $A_{-27}G_{-22}T_{-18}$ were found, the most common being subtype 3.1 associated with
165 *emm*1 and emergent *emm*89, and subtype 3.2 which was found predominantly in the genomes
166 of *emm*4 and *emm*87 and which differed from subtype 3.1 by a single substitution of G for T
167 at -40bp. We measured the activity of NADase in the culture supernatant of strains
168 representing different promoter subtypes and predict that the presence of T/G/C at -40bp does
169 not affect activity of the promoter (Supplementary Figure 3). The fourth promoter variant, $A_{-27}T_{-22}T_{-18}$ is also associated with high activity (15) and was identified in the genomes of
171 *emm*28, *emm*75 and all *emm*78. Only three *emm*-types were exclusively associated with the
172 high activity promoter variant $A_{-27}G_{-22}T_{-18}$; *emm*1, *emm*3 and *emm*12. Other *emm*-types with
173 the high activity promoter variant also had one or more of the other three promoter variants,
174 suggesting a mixed population or, as in the case of *emm*89, an evolving population.

175 To identify any possible recombination events surrounding the P-*nga*-*ifs*-*slo* region, we
176 generated a maximum likelihood phylogeny based on SNPs within the P-*nga*-*ifs*-*slo* (Figure
177 4). This identified several more instances where more than one variant was associated with a
178 single genotype and a cluster of variants with high activity associated promoter residues $A_{-27}G_{-22}T_{-18}$.

180 We sought evidence for acquisition of the high activity-associated promoter $A_{-27}G_{-22}T_{-18}$
181 variant by *emm* genotypes where the dominant or ancestral state was a low activity-associated
182 promoter; these included, in addition to the aforementioned *emm*89: *emm*75, *emm*76, *emm*77,

*emm*81, *emm*82, *emm*87, *emm*94 and *emm*108, all of which are *emm* types frequently identified in the UK and the USA (12-14). Although one *emm*28 was found to carry the high activity-associated promoter, the rest of the *emm*28 population was divided between either $A_{-27}T_{-22}C_{-18}$ or $A_{-27}T_{-22}T_{-18}$ variants. The data pointed to a switch in P-*nga*-*ifs*-*slo* in all cases rather than an *emm* switch, except for *emm*82, where the *emm*82 gene has replaced the *emm*12 gene in an *emm*12 genetic background (14).

High level of mutations within the capsule locus leading to truncations of HasA or HasB

As well as recombination around the P-*nga*-*ifs*-*slo* region, the emergent ST101 variant of *emm*89 had also undergone recombination surrounding the *hasABC* locus, and, in place of the *hasABC* genes, was a region of 156bp that was not found in genotypes with the capsule locus but is found in the acapsular *emm*4 and *emm*22 isolates (3). To identify any similar events in other genotypes, we examined the sequences of *hasA*, *hasB*, and *hasC* in the assemblies of isolates from the BSAC collection as well as CUH (11), PHE-2014/15 and ABCs-2015 collections for gene presence as well as premature stop codon mutations or missing genes (Figure 5). The *hasABC* locus was absent in the majority of *emm*89 isolates, consistent with the previous observations describing the recent emergence of the acapsular *emm*89 variant (3). Similarly, the *hasABC* genes were absent in all *emm*4 and *emm*22 isolates, as previously identified (16), except for two *emm*4 isolates and one *emm*22 isolate which had an intact *hasABC* locus predicted to encode full length proteins. We confirmed the genotypes of these isolates by *emm*-typing the assembled genomes; MLST and phylogenetic analysis indicated they both had a very different genetic background to other *emm*4 or *emm*22 populations suggesting these were not typical of these *emm* types, and therefore they represent examples of *emm* switching. Interestingly, we also identified a similar replacement of *hasABC* for the 156bp region in one *emm*28 isolate (PHE-2014/15, GASEMM1261 (13)), but phylogenetic analysis suggested this was highly divergent to the rest of the *emm*28 population, likely to

represent another example of *emm* switching. Isolated examples of individual *hasA* or *hasB* gene loss were identified in the genomes of isolates belonging to *emm*1 (n=1), *emm*3 (n=1), *emm*11 (n=1), *emm*12 (n=4) and *emm*108 (n=2).

The majority of genotypes (n=35/54, 65%) had isolates without genes or truncation mutations in at least one of *hasABC* genes. In some cases, a consistent mutation could be identified across the genotype (Figure 5). Mutations in *hasC* were rare and only detected in one isolate, an *emm*77 which also had a mutation within *hasA*. Within seven of the eight *emm*-types for which we identified potential P-*nga*-*ifs*-*slo* recombination, a high percentage of isolates had inactivating mutations *hasA* and *hasB* suggesting a possible association between an acapsular and recombination of P-*nga*-*ifs*-*slo*.

Recombination of P-nga-ifs-slo *and surrounding regions*

To confirm our prediction that genotypes *emm*28, *emm*75, *emm*76, *emm*77, *emm*81, *emm*87, *emm*94 and *emm*108 had undergone recombination around P-*nga*-*ifs*-*slo*, we mapped all the genome sequence data for each genotype to the *emm*89 reference genome H293. Gubbins analysis of SNP clustering predicted regions of recombination spanning the *nga*-*ifs*-*slo* region and varying in length in all eight genotypes (Figure 6). To analyse recombination of these genotypes and potential capsule loss further, we studied the population structure of each genotype individually.

Recombination within emm*28 and* emm*87 around P*-nga-ifs-slo *and the capsule locus*

The genotypes *emm*28 and *emm*87 were the sixth and fifth most common in the BSAC collection, and *emm*28 has previously be noted to be a major cause of infection in high income countries (17). We focussed attention on *emm*28 and *emm*87 as there has been little genomic work on these genotypes so far.

All BSAC *emm*28 isolates carried the $A_{-27}T_{-22}C_{-18}$ low activity associated promoter but inclusion of international genomic data identified $A_{-27}T_{-22}T_{-18}$ variant carrying isolates. These two promoter variants were associated with different major lineages within the entire population of 378 international *emm*28 isolates, including one newly sequenced English isolate originally isolated in 1938. The majority of isolates (n=374) clustered either with the reference MGAS6180 strain (USA) (18) or with the reference MEW123 strain (USA) (19) (Figure 7A). Gubbins analysis for core SNP clustering predicted that the two lineages were distinguished by a single 28,200bp region of recombination, between positions 142,426bp (*ntpE*, M28_Spy0126) and 170,625bp (M28_Spy0153) of the MGAS6180 chromosome. This suggests the emergence of one lineage from the other through a single recombination event, followed by expansion of both lineages (Figure 7B). Within the recombination region was the P-*nga-ifs-slo* locus, which differed between the two lineages; although unique in the MGAS6180-like lineage and with low activity associated promoter residues $A_{-27}T_{-22}C_{-18}$, the MEW123-like lineage had a P-*nga-ifs-slo* identical to that found in *emm*78 isolates (Figure 4), with the three key residues of $A_{-27}T_{-22}T_{-18}$. This is supported by recent findings identifying two main lineages within *emm*28 and that the $A_{-27}T_{-22}T_{-18}$ promoter variant conferred greater toxin expression than $A_{-27}T_{-22}C_{-18}$ (15).

Although we identified an $A_{-27}G_{-22}T_{-18}$ high activity variant of P-*nga-ifs-slo* within *emm*28, this was only associated with the highly divergent GASEMM1261 isolate that may represent an *emm* switching event. This isolate, along with three other PHE-2014/15 isolates (GASEMM2648, GASEMM1396 and GASEMM1353) also representing highly divergent lineages, were excluded from the phylogenetic analysis.

All *emm*28 isolates, regardless of lineage and including MGAS6180 (originally isolated in the 1990s), had the same insertion mutation within *hasA* of an A residue after 219 bp. This insertion was predicted to lead to a frameshift and a premature stop codon after 72 amino

acids (aa) instead of full length 420 aa, rendering *hasA* a pseudogene. Some isolates also had additional mutations in *hasA*; a deletion of a A residue in a septa-A tract leading to a frameshift and a stop codon after 7 aa (n=1); a deletion of a T residue in a septa-T tract leading to a frameshift and a stop codon after 15 aa (n=2); an insertion of a A residue after 57 bp leading to a frameshift and a stop codon after 46 aa (n=3). The loss of full length HasA would render the isolates acapsular.

In *emm*28 there were just two exceptions where *hasA* found to be intact: the historical *emm*28 isolate from 1938 had an intact *hasABC* capsule operon; and BSAC_bs2099, which appeared to have undergone recombination to acquire a 22,316bp region surrounding the *hasABC* genes, that was 99% identical to the same region in *emm*2 isolate MGAS10270, suggesting *emm*2 might be the donor for this recombination. Both isolates were predicted to express full length HasA and synthesise capsule. Taken together, in comparison with the oldest *emm*28 isolate, the data showed that post 1930s *emm*28 isolates became acapsular through mutation, but the contemporary population is divided into two major lineages, MEW123-like and MGAS6180-like lineages, that may differ in *nga-ifs-slo* expression. Additionally, there was evidence of geographical structure in the population: the MEW123-like lineage comprised mainly of North American isolates (39/44) and only five from England/Wales; isolates from Australia, France and Lebanon were MGAS6180-like, along with the rest of the England/Wales isolates.

Phylogenetic analysis of the BSAC *emm*87 population was expanded and compared with publicly available *emm*87 genome sequence data, totalling 173 isolates from the UK and North America, including one historical NCTC UK isolate from ~1970-80 (NCTC12065). Gubbins analysis predicted a single 20,506bp region of recombination surrounding the P-*nga-ifs-slo* region, that distinguished the main population from the oldest BSAC isolates from 2001 and the historical 1970-80 NCTC isolate (Figure 7C). Whilst the two 2001 BSAC

281 isolates and the NCTC isolate had a P-*nga-ifs-slo* variant with low activity-associated
282 promoter residues, $G_{27}T_{-22}T_{-18}$, all other *emm*87 isolates had a P-*nga-ifs-slo* region with high
283 activity associated promoter residues, $A_{-27}G_{-22}T_{-18,}$ identical to that found in *emm*4 and some
284 *emm*77. This suggested the emergence of a new lineage through a single recombination event
285 followed by expansion within the population, redolent of that previously observed in *emm*89
286 (Figure 7D).

287 Similar to *emm*28, all *emm*87 isolates, bar four had an insertion of an A residue after 57 bp
288 that resulted in a frameshift mutation in *hasA*, and the introduction of a premature stop codon
289 after 46aa of HasA. This mutation was also identified within the historical NCTC isolate, but
290 was not found in the two 2001 BSAC isolates, that had an intact *hasABC* locus. This mutation
291 was also absent in two PHE-2014/15 isolates that had undergone an additional recombination
292 event (32,243bp) surrounding the *hasABC* locus, although, as this region shared 100% DNA
293 identity to *emm*28 isolate MGAS6180, HasA is truncated. Overall the data showed that, like
294 *emm*89, contemporary *emm*87 are acapsular with a high activity *nga-ifs-slo* promoter,
295 suggesting that this *emm* lineage may have recently shifted towards this genotype/phenotype.

296 *Recombination within different multi-locus sequence types of* emm75

297 The *emm*75 genotype is of interest as a common cause of non-invasive infection in the UK; it
298 is also used in models of nasopharyngeal infection (20, 21). Eleven *emm*75 isolates were
299 present in the BSAC collection, all multilocus sequence type (ST) 150. When we
300 incorporated other available genome sequence data for *emm*75 (n=173), including two newly
301 sequenced historical *emm*75 isolates from 1937 and 1938, two major lineages were identified,
302 characterised by two different MLSTs; ST49 or ST150 (Figure 8A). Although the two
303 historic English isolates were ST49, like the majority of modern North American isolates, the
304 modern England/Wales isolates were predominantly ST150.

Although these two ST lineages differed in the P-*nga-ifs-slo* region there was a high level of predicted recombination across the genomes of both STs, perhaps indicative of historic *emm* switching or extensive genetic exchange. ST49 isolates had the subtype 1.1 low activity $A_{-27}T_{-22}C_{-18}$ promoter, whereas all ST150 isolates had the $A_{-27}G_{-22}T_{-18}$ subtype 3.1 high activity promoter variant, identical to that of *emm*1/*emm*89 (Figure 4). Modern ST49 isolates did, however, differ from historic 1930s isolates by ten distinct regions of predicted recombination (Figure 8B), including a region spanning the *nga-ifs-slo* locus, although this did not include the promoter region. We did not detect any mutations affecting the capsule region in *emm*75. Taken together, *emm*75 was characterised by two major MLST lineages differing in P-*nga/ifs/slo* promoter activity genotypes but without evidence of recent recombination or loss of capsule.

Lineages associated with recombination in emm*76,* emm*77 and* emm*81.*

The phylogeny of all available genome data for *emm*76, *emm*77 and *emm*81 confirmed the presence of diverse lineages, associated with different MLSTs (Figure 9). In all genotypes, however, there was a dominant MLST lineage representing the majority of isolates; ST50 *emm*76, ST63 *emm*77 and ST624 *emm*81. Within the dominant MLST lineages of *emm*76 and *emm*77, there were sub-lineages that were associated with different P-*nga-ifs-slo* variants as well as loss of functional HasA through mutation.

We identified five different MLSTs within *emm*76, but the majority of isolates (30/38) belonged to ST50, including both BSAC isolates. Recombination analysis of the ST50 lineage identified a sub-lineage that differed from other ST50 isolates by 19 regions of recombination (Supplementary Figure 3). One of these regions encompassed P-*nga-ifs-slo*, conferring a P-*nga-ifs-slo* variant closely related to that of modern *emm*1 and *emm*89 with an identical high activity promoter (subtype 3.1). This sub-lineage was dominated by PHE-

329 2014/15 isolates and also contained the more recent of the two BSAC isolates (2008). All
330 isolates in this sub-lineage also had a nonsense mutation within *hasA* of a C to T change at
331 646bp, resulting in a premature stop codon after 215aa, likely to render the isolates acapsular.
332 Only one ST50 isolate outside this sub-lineage had the same *hasA* C646T change. All other
333 *emm*76 isolates would express full length HasA. This suggests the mutation in *hasA* occurred
334 prior to the recombination events.

335 Two sub-lineages were also identified within the dominant *emm*77 lineage ST63, and one
336 was associated with the high activity cluster P-*nga-ifs-slo* variant, compared to predicted low
337 activity variants found in the other *emm*77 lineages. Recombination analysis predicted only
338 two regions of recombination distinguishing the two sub-lineages; a region of 17,954bp
339 surrounding P-*nga-ifs-slo*, and a 173bp region within a hypothetical gene (SPYH293_00394)
340 (Supplementary Figure 4). Whilst all BSAC *emm*77 isolates (years 2001-2009) were ST63
341 with low activity P-*nga-ifs-slo*, PHE isolates from 2014-2015 were almost evenly divided
342 between the two sub-lineages, indicating a potential recent change in England/Wales. All
343 ST63 isolates except three, had a deletion of a T residue within a septa-polyT tract at 458bp
344 in *hasA*, predicted to truncate the HasA protein after 154aa. The three exceptions were
345 predicted to encode full length HasA and were associated with low P-*nga-ifs-slo* promoter
346 activity variants. Although also not associated with high P-*nga-ifs-slo* promoter activity
347 variants, other lineages of *emm*77 also carried mutations within *hasA* that would truncate
348 HasA; ST399 isolates carried an insertion of a T residue at 71 bp of the *hasA* gene resulting
349 in a premature stop codon after 46 aa, and two ST133 isolates carried G894A substitution
350 resulting in a premature stop codon after amino acid residue 297.

351 The *emm*81 population (n=68) was more diverse with nine different sequence types, but the
352 majority of isolates (41/68) were ST624 or the single locus variant ST837 (9/68; one SNP in
353 *recP* allele) within the same lineage (Figure 9). ST171 was restricted to three historical

354 isolates originally collected in 1938-1939. We did not detect any *hasABC* variations that
355 would disrupt translation in *emm*81 lineages except for the dominant group of ST624/ST837,
356 where we identified an A residue insertion at 128 bp in *hasB* resulting in a frameshift and
357 premature stop codon after 50 aa. All ST624/ST837 carried the high activity cluster P-*nga-*
358 *ifs-slo* variant identical to that seen in *emm*3, compared to all other lineages associated with
359 other low activity P-*nga-ifs-slo* variants. Recombination analysis identified extensive
360 recombination had occurred within *emm*81 leading to the different levels of diversity, but we
361 identified one region of recombination that distinguished in the ST624/ST837 lineage
362 compared to the closely related ST909 and ST117 populations (Supplementary Figure 5).
363 This region surrounded the P-*nga-ifs-slo* locus, suggesting ST624/ST837 gained the high
364 activity cluster P- *nga-ifs-slo* variant through recombination, like other *emm*-types,
365 potentially from *emm*3 (Figure 4). The prevalence of the high activity and truncated HasB
366 ST624/ST837 lineage may be a recent event in England/Wales, as all BSAC isolates prior to
367 2009 were outside of this lineage.

368 *High activity cluster P*-nga-ifs-slo *variants gained by recombination in* emm*94 and* emm*108*

369 Within *emm*94, we identified a P-*nga-ifs-slo* identical to that found in *emm*1 with high
370 activity promoter variant subtype 3.1. Phylogenetic analysis of 51 *emm*94 isolates identified a
371 dominant lineage among England/Wales isolates separate to the single USA isolate and two
372 England/Wales isolates (Supplementary Figure 6), that belonged to ST89. Gubbins analysis
373 predicted 11 regions of recombination in all lineage isolates compared to the three outlying
374 isolates, including one (22,648bp) that encompassed P-*nga-ifs-slo*, transferring a high activity
375 $A_{-27}G_{-22}T_{-18}$ P-*nga-ifs-slo* variant. All *emm*94 isolates contained an indel within *hasB*
376 compared to the reference (H293); losing 6bp and gaining 13bp between 127-133bp. This
377 variation causes a frameshift and would truncate the HasB protein after 45aa.

We identified a similar high activity cluster P- *nga-ifs-slo* variant within a single *emm*108 genome originating from the USA. Within the 9 isolates from PHE-2014/15 (n=7) and ABCs-2015 (n=2), there were two sequence types, ST1088 and ST14. ST14 was represented by the only two ABCs-2015 isolates and we identified that both had lost the entire *hasB* gene, although *hasA* and *hasC* were still present (Supplementary Figure 7). Additionally, one of the ABCs-2015 isolates had undergone recombination of a single ~29,683bp region surrounding the P-*nga-ifs-slo*, replacing P-*nga-ifs-slo* for one identical to that found in *emm*3 with high activity promoter variant $A_{-27}G_{-22}T_{-18}$ subtype 3.1.

Discussion

The emergence of new, internationally successful lineages of *S. pyogenes* can be driven by recombination-related genome remodelling, as demonstrated by *emm*1 and *emm*89. The transfer of a P-*nga-ifs-slo* region conferring increased expression to the new variant was common to both genotypes. In the case of *emm*89, five other regions of recombination were identified in the emergent variant, one resulting in the loss of the hyaluronic acid capsule. Although potentially all six regions of recombination combined underpinned the success of the emergent *emm*89, we have shown here that recombination of P-*nga-ifs-slo* has occurred in other leading *emm*-types as well as a high frequency of capsule loss through mutation. These data point to an association between genetic change affecting capsule and recombination affecting the P-*nga-ifs-slo* locus, conferring increased production of *nga-ifs-slo*; in some cases (notably *emm*87, *emm*89, and *emm*94) this has further been associated with an apparent fitness advantage and expansion within the population.

A number of genotypes were found to be associated with multiple variants of P-*nga-ifs-slo*. The majority of genotypes had P-*nga-ifs-slo* variants with the low activity promoter

associated three key residues variants: $G_{-27}T_{-22}T_{-18}$ or $A_{-27}T_{-22}C_{-18}$. Only *emm*1, *emm*3 and *emm*12 were exclusively associated with the high activity $A_{-27}G_{-22}T_{-18}$ variant. We have shown that the same high activity promoter variant is present in isolates belonging to twelve other *emm* types, notably, *emm*76, *emm*77, *emm*81, *emm*87 and *emm*94, although this is not a consistent feature in these genotypes due to *emm*-switching or recombination. We identified four combination of the three key promoter residues and several subtypes of the 67bp promoter that varied in bases other than those at the -27, -22, and -18 key positions. Although some subtypes were restricted to single genotypes, variation in the -40 base led to the subtype 2.2 of $G_{-27}T_{-22}T_{-18}$ and subtype 3.2 of $A_{-27}G_{-22}T_{-18}$. We measured the activity of NADase in representative strains and genotypes of these promoter variants and variation in the -40 base did not impact on the activity conferred by the -27, -22, and -18 bases. Although we predicted the level of *nga* and *slo* expression based on the promoter variant, this may not relate to actual expression given the level of other genetic variation between genotypes. However, our consistent findings of lineages emerging following acquisition of the high activity promoter variant supports the hypothesis that this confers some benefit that may relate to increased toxin expression.

Intriguingly, where we identified an acquisition of the high activity promoter variant through recombination, these genotypes also had a genetic change in the capsule locus, likely rendering the organism unable to make capsule (*hasA* mutation) or only low levels of capsule (*hasB* mutation). To date, only *emm*4, *emm*22, and the emergent *emm*89 lineage are known to lack all three genes required to synthesise capsule. Here, we identified mutations that would truncate HasA and HasB in 35% of all isolates and 65% (35/54) of all genotypes. As the majority of isolates included in this study were invasive or sterile site isolates, the findings further challenge the dogma that the hyaluronan capsule is required for full virulence of *S. pyogenes* and, in addition, lend credence to the possibility that the increased expression of

NADase and SLO may in some way compensate for the lack of capsule (22). While capsule has been shown to underpin resistance to opsonophagocytic killing in the most constitutively hyper-encapsulated genotypes such as *emm*18 (23, 24), there is less evidence that it contributes measurably to opsonophagocytosis killing resistance in other genotypes (3). Whether loss of capsule synthesis is of benefit to *S. pyogenes* is uncertain; the capsule may shield several key adhesins used for interaction with host epithelium and fomites, but may also act as a barrier to transformation with DNA. An accumulation of *hasABC* inactivating mutations have been identified during long term carriage (25) and, although for some genotypes capsule loss impacted on survival in whole human blood, a high number of acapsular *hasA* mutants have also recently been found to be causing a high level of disease in children, including *emm*1, *emm*3 and *emm*12 (26).

The process of recombination in *S. pyogenes* is not well understood and natural competence has only been demonstrated once and under conditions of biofilm or nasopharyngeal infection (27). We do not know if the six regions of recombination that lead to the emergence of the new ST101 *emm*89 variant occurred simultaneously, although no intermediate isolates have been identified. The loss of the hyaluronic acid capsule in the new emergent *emm*89, along with our consistent findings of inactivating mutations associated with P-*nga-ifs-slo* transfer indicate either 1) the process of recombination requires the inactivation of capsule, 2) capsule negative *S. pyogenes* requires high expression of *nga-ifs-slo* for survival, 3) or that capsule negative phenotype combined with high expression of *nga-ifs-slo* provides a greater selective advantage to *S. pyogenes*.

The phylogeny of *emm*28, *emm*87, *emm*76, *emm*77, *emm*94, and *emm*108 indicated that mutations in *hasA* or *hasB* occurred prior to recombination of P-*nga-ifs-slo*, supporting the first hypothesis that prior capsule inactivation is required for recombination. There is no evidence, however, to suggest this was required for recombination in the *emm*1 population. It

could be hypothesised that capsule acts as a barrier to genetic exchange, but there has also been a positive genetic association of capsule to recombination rates (28). A positive association may, however, be related only to species expressing antigenic capsule whereby recombination is required to introduce variation for immune escape.

The *hasC* gene is not essential for capsule synthesis (29) because a paralog of *hasC* exists within the *S. pyogenes* genome. A paralog for *hasB* (*hasB.2*) also exists elsewhere in the *S. pyogenes* chromosome and can act in the absence of *hasB* to produce low levels capsule (30) but *hasA* is absolutely essential for capsule synthesis (29). The mutations in *hasA* in *emm*28 and *emm*87 have been previously noted and confirmed to render the isolates acapsular (26, 31). Not all acapsular isolates were found to carry the high activity promoter of *nga-ifs-slo*, despite being invasive, perhaps refuting the hypothesis that high activity *nga-ifs-slo* promoter is essential for the survival of acapsular *S. pyogenes*.

Interestingly, we identified that the capsule locus is also a target for recombination as, like *emm*89, isolates within *emm*28 and *emm*87 had undergone recombination of this locus and surrounding regions, varying in length (Supplementary Figure 8) and restoring capsule synthesis in *emm*28. Isolated examples of loss of *hasA* or *hasB* genes were identified in some genotypes, such as *emm*108, possibly due to internal recombination and deletion.

Only two *emm*4 and one *emm*22 isolates were found to have P-*nga-ifs-slo* variants that were not an $A_{-27}T_{-22}G_{-18}$ high activity promoter variants, and interestingly these isolates carried the *hasABC* genes, typically absent in *emm*4 and *emm*22. The high genetic distance of these isolates to the other *emm*4 and *emm*22 genomes indicated potentially *emm* switching of the *emm*4 or *emm*22 genes onto different genetic backgrounds. The single *emm*28 with a high activity P-*nga-ifs-slo* variant also may be an example of this, and was one of four *emm*28 isolates that did not cluster with the two main *emm*28 lineages. Although we excluded them

476 from our analysis as we focussed on recombination within the two main lineages, this
477 potential for highly diverse variants within genotypes and the potential for *emm*-switching
478 warrants further investigation, particularly as the most promising current vaccine is multi-
479 valent towards common M types (32).

480 All other genotypes carrying the high activity P-*nga*-*ifs*-*slo* variant were found to have
481 undergone recombination of this region; *emm*28, *emm*75, *emm*76, *emm*77, *emm*81, *emm*87,
482 *emm*94 and *emm*108, as well as the previously described *emm*1 and *emm*89.

483 Within *emm*87, we identified three isolates outside of the main population lineage that
484 represented the oldest isolates in the collection; two from 2001 (different geographical
485 locations within England) and one from ~1970-80. A single region of recombination,
486 surrounding the P-*nga*-*ifs*-*slo* locus distinguished the main population lineage from the three
487 older isolates, consistent with a recombination event but, due to a lack of earlier isolates of
488 *emm*87, we could not confirm a recombination related shift in the population, as reported
489 previously for *emm*89 and *emm*1.

490 The existence of two lineages within the contemporary *emm*28 suggests that one has not yet
491 displaced the other, although the MEW123-like lineage was predominantly USA isolates,
492 consistent with recent findings (15). The P-*nga*-*ifs*-*slo* region with the high activity associated
493 $A_{-27}T_{-22}T_{-18}$ and acquired through recombination by the MEW123-like lineage was identical
494 to that found in *emm*78, indicating *emm*78 as the potential genetic donor. We found *emm*78 to
495 have high levels of NADase activity, as predicted, and interestingly, like *emm*28, all eight
496 *emm*78 isolates were acapsular due to a deletion within the *hasABC* promoter region
497 extending into *hasA*. This again may support the hypothesis that capsule negative *S. pyogenes*
498 requires high expression of *nga*-*ifs*-*slo* for survival.

A strength of this study was the systematic longitudinal sampling over a 10 year period; as expected, this again identified the shift in the *emm*89 population. Other *emm*-types exhibited lineages with different P-*nga*-*ifs*-*slo* variants, and those with the more active promoter variant did appear to become dominant over time, similar to *emm*1 and the emergent *emm*89 lineages. For example, the high activity P-*nga*-*ifs*-*slo* ST63 lineage of *emm*77 was not detected in England/Wales isolates prior to 2014-15. Similarly, the high activity P-*nga*-*ifs*-*slo* variant *emm*81 ST646/ST837 lineage was represented by only a single isolate (of six) collected 2001-2009 but became dominant by 2014/15 in England/Wales and the USA. *emm*75 was the 6th most common genotype in England/Wales 2014-15 and dominated by high activity P-*nga*-*ifs*-*slo* variant ST150 lineage, yet less common in the USA where ST49 with low activity P-*nga*-*ifs*-*slo* is dominant. A high prevalence of *emm*94 was also found in England/Wales 2014-15 but was rare in the USA (only 1 isolate). Our analysis of this genotype indicated there has been a recombination related change in the population as we detected 11 regions of predicted recombination including P-*nga*-*ifs*-*slo* potentially conferring high toxin expression. The other ten regions of recombination may also provide advantages to this lineage along with a potential low level of capsule through *hasB* mutation.

The development and boosting of circulating antibodies to SLO is often used as a diagnostic biomarker of recent *S. pyogenes* infection and is known to be more specific to throat rather than skin infections. The genomic analysis provides explanation for this historic and well-recognized association between anti- SLO titres and disease patterns, due to known tissue tropism of *S. pyogenes emm* types. Whether the alteration of SLO activity in different *S. pyogenes* strains might render such a test more or less specific will be of interest, although may explain observed differences in ASO titre between genotypes (33). There is also the possibility that other beta haemolytic streptococci might acquire similarly active SLO production, reducing the specificity of ASO titre to *S. pyogenes*.

524 Our genomic analysis has uncovered convergent evolutionary pathways towards capsule loss
525 and recombination related re-modelling of the P-*nga-ifs-slo* locus in leading contemporary
526 genotypes. This suggests that a combination of capsule loss and gain of high *nga-ifs-slo*
527 expression provides a greater selective advantage than either of these phenotypes alone.
528 Acquisition of the high activity promoter led to pandemic *emm*1 and *emm*89 clones that are
529 dominant and highly successful. Active surveillance of the lineages comprising *emm*76,
530 *emm*77, *emm*81, *emm*87, *emm*94 and *emm*108 is required to determine if capsule
531 loss/reduction and recombination of P-*nga-ifs-slo* towards high expression will trigger
532 expansion towards additional pandemic clones in the next few years.

533 **Materials & Methods**

534 **Isolates**

535 344 isolates of *S. pyogenes* associated with blood stream infections and submitted to the
536 British Society for Antimicrobial Chemotherapy (BSAC, www.bsacsurv.org) from 11
537 different sites across the UK between 2001-2011 were subjected to whole genome
538 sequencing (Supplementary Table 1). All BSAC isolates were tested for antibiotic
539 susceptibility using the BSAC agar dilution method to determine MICs (34).

540 A further six isolates were sequenced from a historical collection of *S. pyogenes* originally
541 collected in the 1930s from puerperal sepsis patients at Queen Charlottes Hospital, London,
542 UK; one *emm*28 from 1938 (ERR485803), two *emm*75 from 1937 (ERR485807) and 1939
543 (ERR485820), three *emm*81 from 1938 (ERR485805) and 1939 (ERR485801, ERR485802).

544 **Genome sequencing**

545 Streptococcal DNA was extracted using the QIAxtractor instrument according to the
546 manufacturer's instructions (QIAgen, Hilden, Germany), or manually using a phenol-
547 chloroform method (35). DNA library preparation was conducted according to the

548 Illumina protocol and sequencing was performed on an Illumina HiSeq 2000 with 100-
549 cycle paired-end runs. Sequence data have been submitted to the European Nucleotide
550 Archive (ENA) (www.ebi.ac.uk/ena) (accession numbers in Supplementary Table 2).

551 Genomes were *de novo* assembled using Velvet with the pipeline and improvements found
552 at https://github.com/sanger-pathogens/vr-codebase and https://github.com/sanger-
553 pathogens/assembly_improvement (36). Annotation was performed using Prokka. *emm*
554 genotypes were determined from the assemblies and multilocus sequence types (MLSTs)
555 were identified using the MLST database (pubmlst.org/spyogenes) and an in-house script
556 (https://github.com/sanger-pathogens/mlst_check). New MLST were submitted to the
557 database (https://pubmlst.org/). Antimicrobial resistance genes were identified by srst2
558 (37) using the ARG-ANNOT database (ARGannot_r2.fasta) (38).

559 **Genome sequence analysis**

560 Sequence reads were mapped using SMALT (https://www.sanger.ac.uk/science/tools/smalt)
561 to the completed *emm*89 reference genome H293 (3) as this genome contains no known
562 prophage regions. Other reference genomes were also used where indicated with predicted
563 prophage regions (Supplementary Table 3) excluded to obtain 'core' SNPs. Maximum-
564 likelihood phylogenetic trees were generated from aligned core SNPs using RAxML (39)
565 with the GTR substitution model (39) and 100 bootstraps. Regions of recombination were
566 predicted using Gubbins analysis using the default parameters (40).

567 Other genome sequence data were obtained from the short read archive. We combined data
568 collected across England and Wales through Public Health England during 2014 and 2015
569 (PHE-2014/15) supplied by Kapatai *et al*. (13) and Chalker *et al*. (12) from invasive and non-
570 invasive *S. pyogenes* isolates. We also used data supplied by Chochua et al. (14) collected by
571 Active Bacterial Core Surveillance USA in 2015 (ABCs-2015) from invasive *S. pyogenes*

572 isolates. ABCs-2015 sequence data was pre-processed by Trimmomatic (41) to remove
573 adapters and low quality sequences. PHE-2014/15 had already been pre-processed (12, 13).
574 Genome data from these collections were assembled *de novo* using Velvet (assembly
575 statistics provided in Supplementary Table 2) and any isolates with atypical total assembled
576 length or contig numbers were excluded. We also used data from Turner *et al*. (2017) of
577 invasive and non-invasive isolates from the Cambridgeshire region, UK and collected
578 through Cambridge University Hospital (CUH) (11). We relied on the *emm*-type determined
579 during the original studies and excluded any data where the *emm*-type was uncertain or
580 negative. The genes *hasA*, *hasB*, *hasC* and the P-*nga-ifs-slo* were extracted from the
581 assembled genome using *in silico* PCR (https://github.com/simonrharris/in_silico_pcr).
582 Capsule locus and P-*nga-ifs-slo* variants were also confirmed through mapping.

583 **NADase activity**

584 Activity of NADase was measured in culture supernatant as previously described (3).
585 Activity was determined as the highest dilution capable of hydrolysing NAD+.

586 **Conflict of interest**

587 SJP is a consultant to Specific and Next Gen Diagnostics.

588 **Acknowledgments**

589 This publication presents independent research supported by the Health Innovation Challenge
590 Fund (WT098600, HICF-T5-342), a parallel funding partnership between the Department of
591 Health and Wellcome Trust. The work was also funded by the UK Clinical Research
592 Collaboration (UKCRC, National centre for Infection Prevention & Management) and the
593 National Institute for Health Research Biomedical Research Centre awarded to Imperial
594 College London. The views expressed in this publication are those of the author(s) and not
595 necessarily those of the Department of Health, NIHR, or Wellcome Trust. CET was an

596 Imperial College Junior Research Fellow and is a Royal Society & Wellcome Trust Sir Henry

597 Dale Fellow (208765/Z/17/Z).

598

599

References

1. **Nasser W, Beres SB, Olsen RJ, Dean MA, Rice KA, Long SW, Kristinsson KG, Gottfredsson M, Vuopio J, Raisanen K, Caugant DA, Steinbakk M, Low DE, McGeer A, Darenberg J, Henriques-Normark B, Van Beneden CA, Hoffmann S, Musser JM.** 2014. Evolutionary pathway to increased virulence and epidemic group A *Streptococcus* disease derived from 3,615 genome sequences. *Proc Natl Acad Sci U S A* **111:**E1768-1776.

2. **Zhu L, Olsen RJ, Nasser W, Beres SB, Vuopio J, Kristinsson KG, Gottfredsson M, Porter AR, DeLeo FR, Musser JM.** 2015. A molecular trigger for intercontinental epidemics of group A *Streptococcus*. *J Clin Invest* **125:**3545-3559.

3. **Turner CE, Abbott J, Lamagni T, Holden MT, David S, Jones MD, Game L, Efstratiou A, Sriskandan S.** 2015. Emergence of a new highly successful acapsular group A *Streptococcus* clade of genotype *emm*89 in the United Kingdom. *MBio* **6:**e00622.

4. **Zhu L, Olsen RJ, Nasser W, de la Riva Morales I, Musser JM.** 2015. Trading capsule for increased cytotoxin production: contribution to virulence of a newly emerged clade of *emm*89 *Streptococcus pyogenes*. *MBio* **6:**e01378-01315.

5. **Beres SB, Olsen RJ, Ojeda Saavedra M, Ure R, Reynolds A, Lindsay DSJ, Smith AJ, Musser JM.** 2017. Genome sequence analysis of *emm*89 *Streptococcus pyogenes* strains causing infections in Scotland, 2010-2016. *J Med Microbiol* **66:**1765-1773.

6. **Friaes A, Machado MP, Pato C, Carrico J, Melo-Cristino J, Ramirez M.** 2015. Emergence of the same successful clade among distinct populations of *emm*89 *Streptococcus pyogenes* in multiple geographic regions. *MBio* **6:**e01780-01715.

7. **Latronico F, Nasser W, Puhakainen K, Ollgren J, Hyyrylainen HL, Beres SB, Lyytikainen O, Jalava J, Musser JM, Vuopio J.** 2016. Genomic characteristics

behind the spread of bacteremic group A *Streptococcus* Type *emm*89 in Finland, 2004-2014. *J Infect Dis* **214:**1987-1995.

8. **Hasegawa T, Hata N, Matsui H, Isaka M, Tatsuno I.** 2017. Characterisation of clinically isolated *Streptococcus pyogenes* from balanoposthitis patients, with special emphasis on *emm*89 isolates. *J Med Microbiol* **66:**511-516.

9. **Kimoto H, Fujii Y, Yokota Y, Taketo A.** 2005. Molecular characterization of NADase-streptolysin O operon of hemolytic streptococci. *Biochim Biophys Acta* **1681:**134-149.

10. **Sumby P, Porcella SF, Madrigal AG, Barbian KD, Virtaneva K, Ricklefs SM, Sturdevant DE, Graham MR, Vuopio-Varkila J, Hoe NP, Musser JM.** 2005. Evolutionary origin and emergence of a highly successful clone of serotype M1 group A *Streptococcus* involved multiple horizontal gene transfer events. *J Infect Dis* **192:**771-782.

11. **Turner CE, Bedford L, Brown NM, Judge K, Torok ME, Parkhill J, Peacock SJ.** 2017. Community outbreaks of group A *Streptococcus* revealed by genome sequencing. *Sci Rep* **7:**8554.

12. **Chalker V, Jironkin A, Coelho J, Al-Shahib A, Platt S, Kapatai G, Daniel R, Dhami C, Laranjeira M, Chambers T, Guy R, Lamagni T, Harrison T, Chand M, Johnson AP, Underwood A, Scarlet Fever Incident Management T.** 2017. Genome analysis following a national increase in Scarlet Fever in England 2014. *BMC Genomics* **18:**224.

13. **Kapatai G, Coelho J, Platt S, Chalker VJ.** 2017. Whole genome sequencing of group A *Streptococcus*: development and evaluation of an automated pipeline for emmgene typing. *PeerJ* **5:**e3226.

649 14. **Chochua S, Metcalf BJ, Li Z, Rivers J, Mathis S, Jackson D, Gertz RE, Jr.,**
650 **Srinivasan V, Lynfield R, Van Beneden C, McGee L, Beall B.** 2017. Population and
651 whole genome sequence based characterization of invasive group A streptococci
652 recovered in the United States during 2015. *MBio* **8**.
653 15. **Kachroo P, Eraso JM, Beres SB, Olsen RJ, Zhu L, Nasser W, Bernard PE, Cantu**
654 **CC, Saavedra MO, Arredondo MJ, Strope B, Do H, Kumaraswami M, Vuopio J,**
655 **Grondahl-Yli-Hannuksela K, Kristinsson KG, Gottfredsson M, Pesonen M,**
656 **Pensar J, Davenport ER, Clark AG, Corander J, Caugant DA, Gaini S,**
657 **Magnussen MD, Kubiak SL, Nguyen HAT, Long SW, Porter AR, DeLeo FR,**
658 **Musser JM.** 2019. Integrated analysis of population genomics, transcriptomics and
659 virulence provides novel insights into *Streptococcus pyogenes* pathogenesis. *Nat Genet*
660 **51:**548-559.
661 16. **Flores AR, Jewell BE, Fittipaldi N, Beres SB, Musser JM.** 2012. Human disease
662 isolates of serotype m4 and m22 group A *Streptococcus* lack genes required for
663 hyaluronic acid capsule biosynthesis. *MBio* **3:**e00413-00412.
664 17. **Steer AC, Law I, Matatolu L, Beall BW, Carapetis JR.** 2009. Global *emm* type
665 distribution of group A streptococci: systematic review and implications for vaccine
666 development. *Lancet Infect Dis* **9:**611-616.
667 18. **Green NM, Zhang S, Porcella SF, Nagiec MJ, Barbian KD, Beres SB, LeFebvre**
668 **RB, Musser JM.** 2005. Genome sequence of a serotype M28 strain of group A
669 *Streptococcus*: potential new insights into puerperal sepsis and bacterial disease
670 specificity. *J Infect Dis* **192:**760-770.
671 19. **Jacob KM, Spilker T, LiPuma JJ, Dawid SR, Watson ME, Jr.** 2016. Complete
672 genome sequence of *emm*28 type *Streptococcus pyogenes* MEW123, a Streptomycin-

673 Resistant derivative of a clinical throat isolate suitable for investigation of pathogenesis.
674 *Genome Announc* **4**.
675 20. **Alam FM, Turner CE, Smith K, Wiles S, Sriskandan S.** 2013. Inactivation of the
676 CovR/S virulence regulator impairs infection in an improved murine model of
677 *Streptococcus pyogenes* naso-pharyngeal infection. *PLoS One* **8:**e61655.
678 21. **Osowicki J, Azzopardi KI, McIntyre L, Rivera-Hernandez T, Ong CY, Baker C,**
679 **Gillen CM, Walker MJ, Smeesters PR, Davies MR, Steer AC.** 2019. A controlled
680 human infection model of group A *Streptococcus* pharyngitis: Which Strain and Why?
681 *mSphere* **4**.
682 22. **Sierig G, Cywes C, Wessels MR, Ashbaugh CD.** 2003. Cytotoxic effects of
683 streptolysin O and streptolysin S enhance the virulence of poorly encapsulated group A
684 streptococci. *Infect Immun* **71:**446-455.
685 23. **Lynskey NN, Goulding D, Gierula M, Turner CE, Dougan G, Edwards RJ,**
686 **Sriskandan S.** 2013. RocA truncation underpins hyper-encapsulation, carriage
687 longevity and transmissibility of serotype M18 group A streptococci. *PLoS Pathog*
688 **9:**e1003842.
689 24. **Moses AE, Wessels MR, Zalcman K, Alberti S, Natanson-Yaron S, Menes T,**
690 **Hanski E.** 1997. Relative contributions of hyaluronic acid capsule and M protein to
691 virulence in a mucoid strain of the group A *Streptococcus*. *Infect Immun* **65:**64-71.
692 25. **Flores AR, Jewell BE, Olsen RJ, Shelburne SA, 3rd, Fittipaldi N, Beres SB,**
693 **Musser JM.** 2014. Asymptomatic carriage of group A *Streptococcus* is associated with
694 elimination of capsule production. *Infect Immun* **82:**3958-3967.
695 26. **Flores AR, Chase McNeil J, Shah B, Van Beneden C, Shelburne SA, 3rd.** 2018.
696 Capsule-negative *emm* types are an increasing cause of pediatric group A streptococcal

infections at a large pediatric hospital in Texas. *J Pediatric Infect Dis Soc* doi:10.1093/jpids/piy053.

27. **Marks LR, Mashburn-Warren L, Federle MJ, Hakansson AP.** 2014. *Streptococcus pyogenes* biofilm growth in vitro and in vivo and its role in colonization, virulence, and genetic exchange. *J Infect Dis* **210:**25-34.

28. **Rendueles O, de Sousa JAM, Bernheim A, Touchon M, Rocha EPC.** 2018. Genetic exchanges are more frequent in bacteria encoding capsules. *PLoS Genet* **14:**e1007862.

29. **Ashbaugh CD, Alberti S, Wessels MR.** 1998. Molecular analysis of the capsule gene region of group A *Streptococcus*: the *hasAB* genes are sufficient for capsule expression. *J Bacteriol* **180:**4955-4959.

30. **Cole JN, Aziz RK, Kuipers K, Timmer AM, Nizet V, van Sorge NM.** 2012. A conserved UDP-glucose dehydrogenase encoded outside the *hasABC* operon contributes to capsule biogenesis in group A *Streptococcus*. *J Bacteriol* **194:**6154-6161.

31. **Tagini F, Aubert B, Troillet N, Pillonel T, Praz G, Crisinel PA, Prod'hom G, Asner S, Greub G.** 2017. Importance of whole genome sequencing for the assessment of outbreaks in diagnostic laboratories: analysis of a case series of invasive *Streptococcus pyogenes* infections. *Eur J Clin Microbiol Infect Dis* **36:**1173-1180.

32. **Steer AC, Carapetis JR, Dale JB, Fraser JD, Good MF, Guilherme L, Moreland NJ, Mulholland EK, Schodel F, Smeesters PR.** 2016. Status of research and development of vaccines for *Streptococcus pyogenes*. *Vaccine* **34:**2953-2958.

33. **Johnson DR, Kurlan R, Leckman J, Kaplan EL.** 2010. The human immune response to streptococcal extracellular antigens: clinical, diagnostic, and potential pathogenetic implications. *Clin Infect Dis* **50:**481-490.

34. **Reynolds R, Hope R, Williams L, Surveillance BWPoR.** 2008. Survey, laboratory and statistical methods for the BSAC Resistance Surveillance Programmes. *J Antimicrob Chemother* **62 Suppl 2:**ii15-28.

35. **Pospiech A, Neumann B.** 1995. A versatile quick-prep of genomic DNA from gram-positive bacteria. *Trends Genet* **11:**217-218.

36. **Page AJ, De Silva N, Hunt M, Quail MA, Parkhill J, Harris SR, Otto TD, Keane JA.** 2016. Robust high-throughput prokaryote de novo assembly and improvement pipeline for Illumina data. *Microb Genom* **2:**e000083.

37. **Inouye M, Dashnow H, Raven LA, Schultz MB, Pope BJ, Tomita T, Zobel J, Holt KE.** 2014. SRST2: Rapid genomic surveillance for public health and hospital microbiology labs. *Genome Med* **6:**90.

38. **Gupta SK, Padmanabhan BR, Diene SM, Lopez-Rojas R, Kempf M, Landraud L, Rolain JM.** 2014. ARG-ANNOT, a new bioinformatic tool to discover antibiotic resistance genes in bacterial genomes. *Antimicrob Agents Chemother* **58:**212-220.

39. **Stamatakis A.** 2014. RAxML version 8: a tool for phylogenetic analysis and post-analysis of large phylogenies. *Bioinformatics* **30:**1312-1313.

40. **Croucher NJ, Page AJ, Connor TR, Delaney AJ, Keane JA, Bentley SD, Parkhill J, Harris SR.** 2015. Rapid phylogenetic analysis of large samples of recombinant bacterial whole genome sequences using Gubbins. *Nucleic Acids Res* **43:**e15.

41. **Bolger AM, Lohse M, Usadel B.** 2014. Trimmomatic: a flexible trimmer for Illumina sequence data. *Bioinformatics* **30:**2114-2120.

42. **Athey TB, Teatero S, Li A, Marchand-Austin A, Beall BW, Fittipaldi N.** 2014. Deriving group A *Streptococcus* typing information from short-read whole-genome sequencing data. *J Clin Microbiol* **52:**1871-1876.

744 43. **Long SW, Kachroo P, Musser JM, Olsen RJ.** 2017. Whole-Genome sequencing of a
745 human clinical isolate of *emm*28 *Streptococcus pyogenes* causing necrotizing fasciitis
746 acquired contemporaneously with Hurricane Harvey. *Genome Announc* **5**.
747 44. **Ibrahim J, Eisen JA, Jospin G, Coil DA, Khazen G, Tokajian S.** 2016. Genome
748 analysis of *Streptococcus pyogenes* associated with pharyngitis and skin infections.
749 *PLoS One* **11:**e0168177.
750 45. **Ben Zakour NL, Venturini C, Beatson SA, Walker MJ.** 2012. Analysis of a
751 *Streptococcus pyogenes* puerperal sepsis cluster by use of whole-genome sequencing.
752 *J Clin Microbiol* **50:**2224-2228.
753 46. **de Andrade Barboza S, Meygret A, Vincent P, Moullec S, Soriano N, Lagente V,**
754 **Minet J, Kayal S, Faili A.** 2015. Complete Genome Sequence of Noninvasive
755 *Streptococcus pyogenes* M/*emm*28 Strain STAB10015, Isolated from a Child with
756 Perianal Dermatitis in French Brittany. *Genome Announc* **3**.
757 47. **Longo M, De Jode M, Plainvert C, Weckel A, Hua A, Chateau A, Glaser P, Poyart**
758 **C, Fouet A.** 2015. Complete Genome Sequence of *Streptococcus pyogenes emm*28
759 Clinical Isolate M28PF1, Responsible for a Puerperal Fever. *Genome Announc* **3**.
760 48. **Athey TB, Teatero S, Sieswerda LE, Gubbay JB, Marchand-Austin A, Li A,**
761 **Wasserscheid J, Dewar K, McGeer A, Williams D, Fittipaldi N.** 2016. High
762 Incidence of Invasive Group A *Streptococcus* Disease Caused by Strains of Uncommon
763 emm Types in Thunder Bay, Ontario, Canada. *J Clin Microbiol* **54:**83-92.
764 49. **Flores AR, Luna RA, Runge JK, Shelburne SA, 3rd, Baker CJ.** 2017. Cluster of
765 Fatal Group A streptococcal *emm*87 infections in a single family: molecular basis for
766 invasion and transmission. *J Infect Dis* **215:**1648-1652.
767 50. **Rochefort A, Boukthir S, Moullec S, Meygret A, Adnani Y, Lavenier D, Faili A,**
768 **Kayal S.** 2017. Full sequencing and genomic analysis of three *emm*75 group A

769 *Streptococcus* strains recovered in the course of an epidemiological shift in French
770 Brittany. *Genome Announc* **5**.

771

772

773 **Tables**

774 **Table 1. Three key residue variants within the *nga-ifs-slo* promoter**

Promoter variant	Type	Genotype (% of isolates)
$A_{-27}T_{-22}C_{-18}$	1.1	**4 (1)***, 8 (100), **9 (92)**, 11 (100), **22 (3)**, **25 (33)**, **28 (87.7)**, 33 (100), 41 (100), 43 (100), **44 (9)**, 49 (100), 53 (100), **58 (15)**, 60 (100), 63 (100), **75 (9)**, **76 (41)**, **77 (29)**, **81 (23)**, **82 (1)**, **88 (33)**, **89 (1)**, **90 (4)**, 92 (100), **94 (6)**, 101 (100), **102 (50)**, **103 (17)**, 106 (100), **108 (89)**, 110 (100), 113 (100), 151 (100), 168 (100), 232 (100)
	1.2	9(8)
	1.3	88(67)
$G_{-27}T_{-22}T_{-18}$	2.1	5 (100), 6 (100), 18 (100), **25 (67)**, **44 (28)**, 68 (100), **75 (1)**, **76 (5), 77 (1), 82 (1), 87 (2), 89 (6), 90 (96),** 91 (100)**, 102 (50), 103 (83),** 104 (100),
	2.2	118 (100) 2 (100), 27 (100), **44 (62)**, **58 (85)**, 59 (100), 73 (100), **76 (11)**, **77 (36)**, **82 (89)**, 83 (100)
	2.3	32 (100)
$A_{-27}G_{-22}T_{-18}$	3.1	1(100), 3 (100), 12 (100), **22 (97)**, **75 (90)**, **76 (43)**, **81 (77)**, **82 (9)**, **89 (93)**, **94 (94)**, **108 (11)**
	3.2	**4 (99), 28 (0.3), 77 (34)**, **87 (98)**
$A_{-27}T_{-22}T_{-18}$	4	**28 (12)**, 78 (100)

775 * genotypes in bold have more than one variant within the population

776

777

778 **Figures**

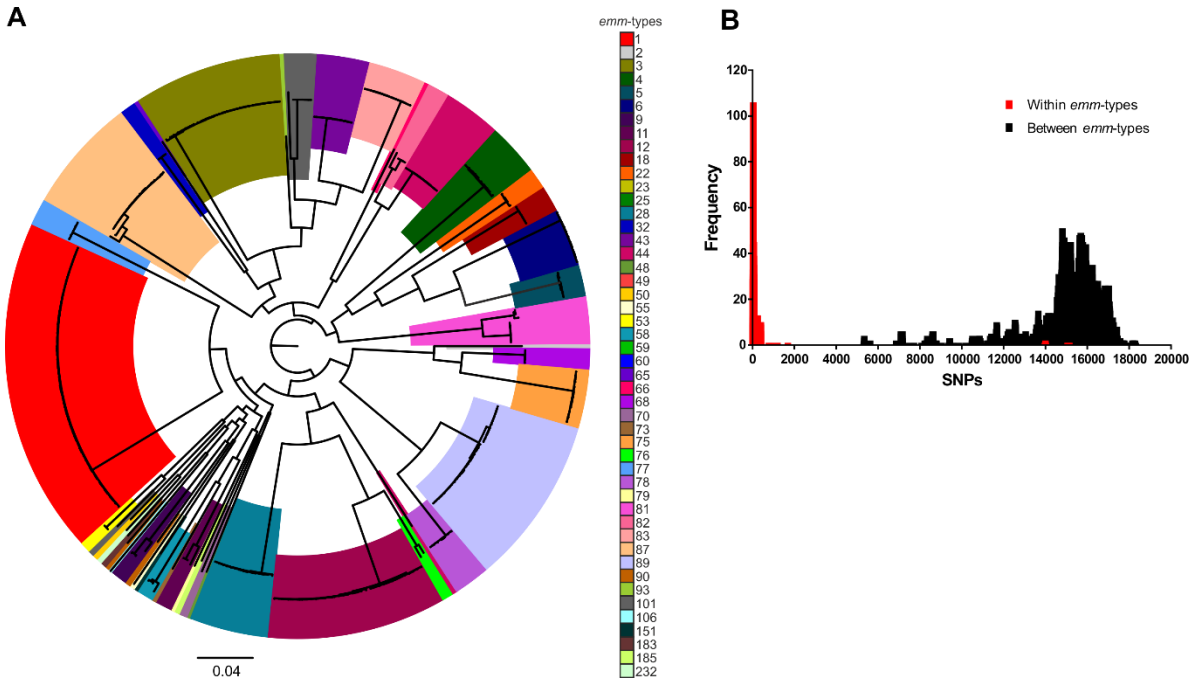

779

780 **Figure 1. Low diversity within *emm* genotypes.** (**A**) A maximum likelihood phylogenetic
781 tree constructed from core SNPs extracted after mapping all 344 BSAC isolates to the
782 complete reference strain H293, identified that the majority of isolates cluster by *emm*
783 genotype. Exceptions were *emm*44, *emm*90 and *emm*101, each of which were present as two
784 separate lineages. (**B**) As reflected by the phylogenetic tree, the number of SNPs separating
785 isolates was high (>5000) when the genomes of isolates of different *emm*-types were
786 compared (black bars). This was much lower when comparisons were made between the
787 genomes of isolates of the same *emm*-type (red bars).

788

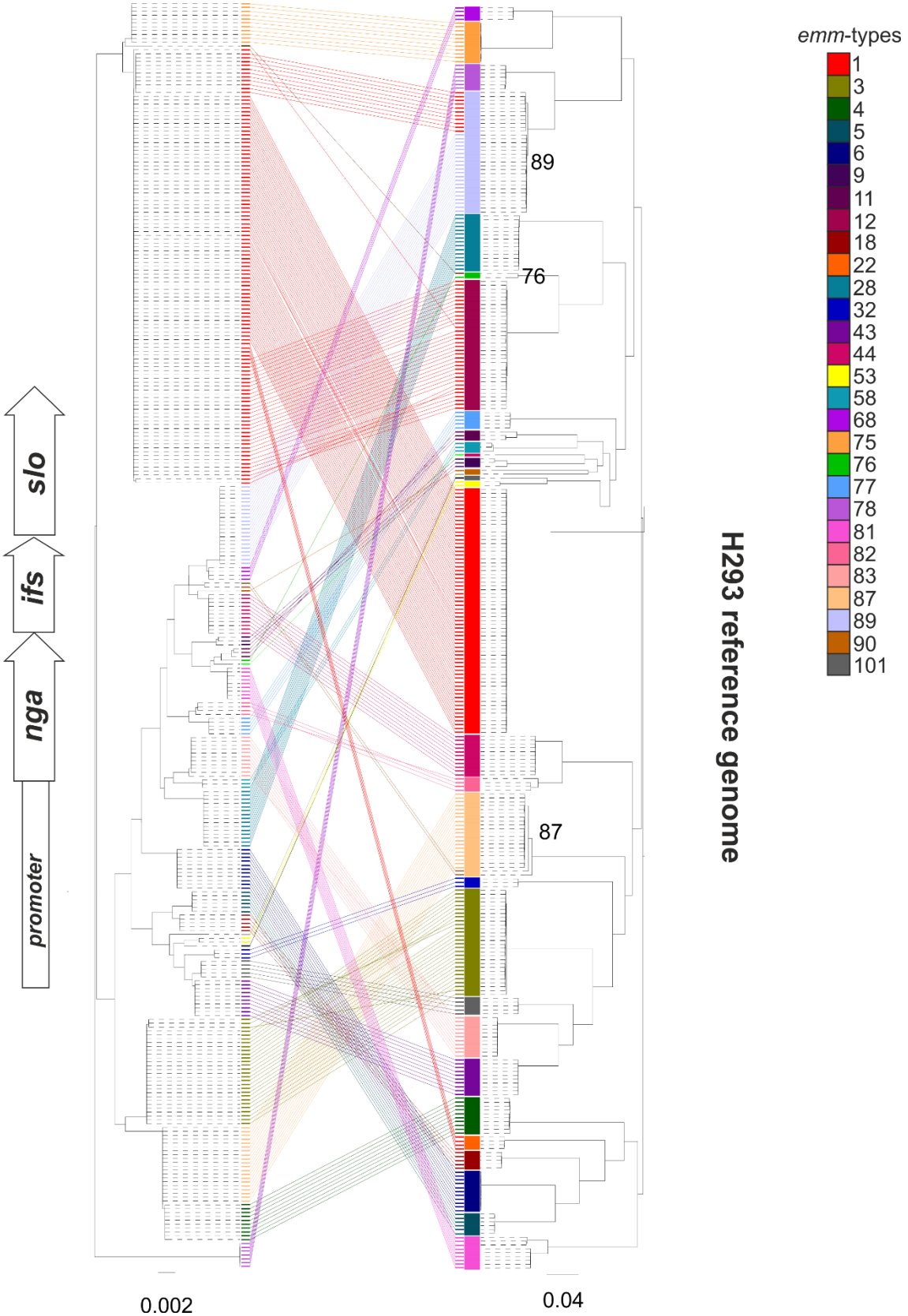

Figure 2. Comparison of the variation within the P-*nga*-*ifs*-*slo* region and core chromosome. A maximum likelihood phylogenetic tree was constructed from SNPs

792 extracted from an alignment of the *nga-ifs-slo* locus and associated upstream region to
793 include the promoter (P-*nga-ifs-slo*) extracted from *de novo* assemblies of 344 BSAC *S.*
794 *pyogenes* (Left tree). This was compared to the phylogenetic tree constructed using SNPs
795 across the entire genome after mapping to the H293 reference genome (Right tree). Only
796 *emm* genotypes represented by two or more isolates were included. Coloured blocks on the
797 right tree represent *emm*-type. Variants of the P-*nga-ifs-slo* are of the same colour if unique to
798 that genotype. The P-*nga-ifs-slo* variant found in *emm*1 (red) was common to other genotypes
799 *emm*12, *emm*22 and some *emm*89. The genotypes *emm*76, *emm*87 and *emm*89 are indicated
800 as they are linked to more than one variant of P-*nga-ifs-slo*. Scale bar represents substitution
801 per site.

802

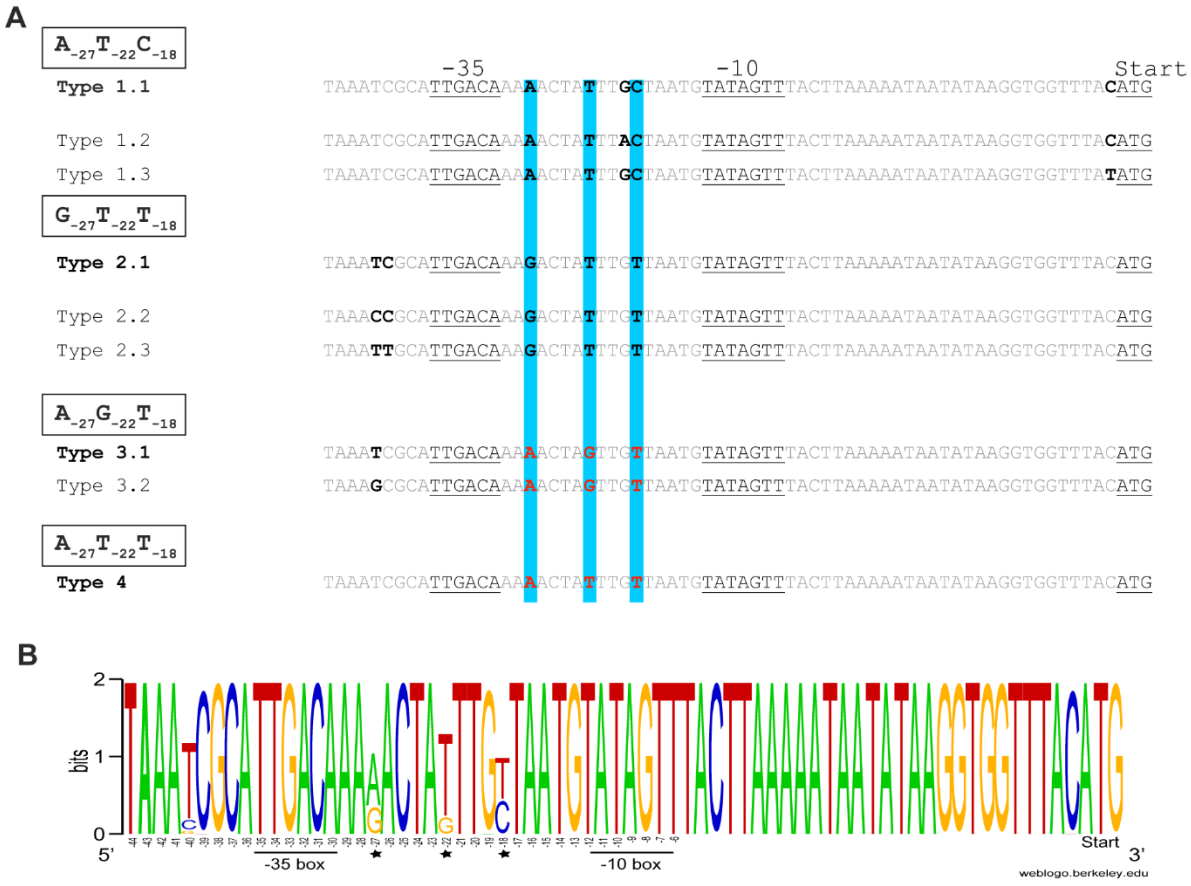

Figure 3. Variants of the *nga-ifs-slo* promoter. (A) The three key residues predicted to influence promoter activity are highlighted blue with those associated with high activity in red. We identified four combinations of these residues (four promoter types) with subtype variants differing in residues other than -27, -22 and -18 (residue positions relative to the underlined -35 and -10 regions) in the predicted 67bp promoter region (9). The combination of $A_{-27}T_{-22}C_{-18}$ subtype 1.1 in historical *emm*1 and $G_{-27}T_{-22}T_{-18}$ subtype 2.1 in older *emm*89 have been shown to be associated with low level promoter activity. $A_{-27}G_{-22}T_{-18}$ subtype 3.1 promoter in modern *emm*1 and emergent variant *emm*89 has been shown to have high activity. $A_{-27}T_{-22}T_{-18}$ subtype 4 promoter has also been shown to have high activity in *emm*28 (15). Subtypes 1.2, 1.3 and 2.3 were restricted to *emm*9, *emm*88 and *emm*32 strains respectively. **(B)** Weblogo representation of the variability in the 67bp promoter region of *nga/ifs/slo* within the 54 different *emm*-types. Key residues -27, -22, -18 are highlighted (star)

816 and their positions are relative to the -35 and -10 boxes. Figure generated using

817 weblogo.berkeley.edu.

818

819

820

821

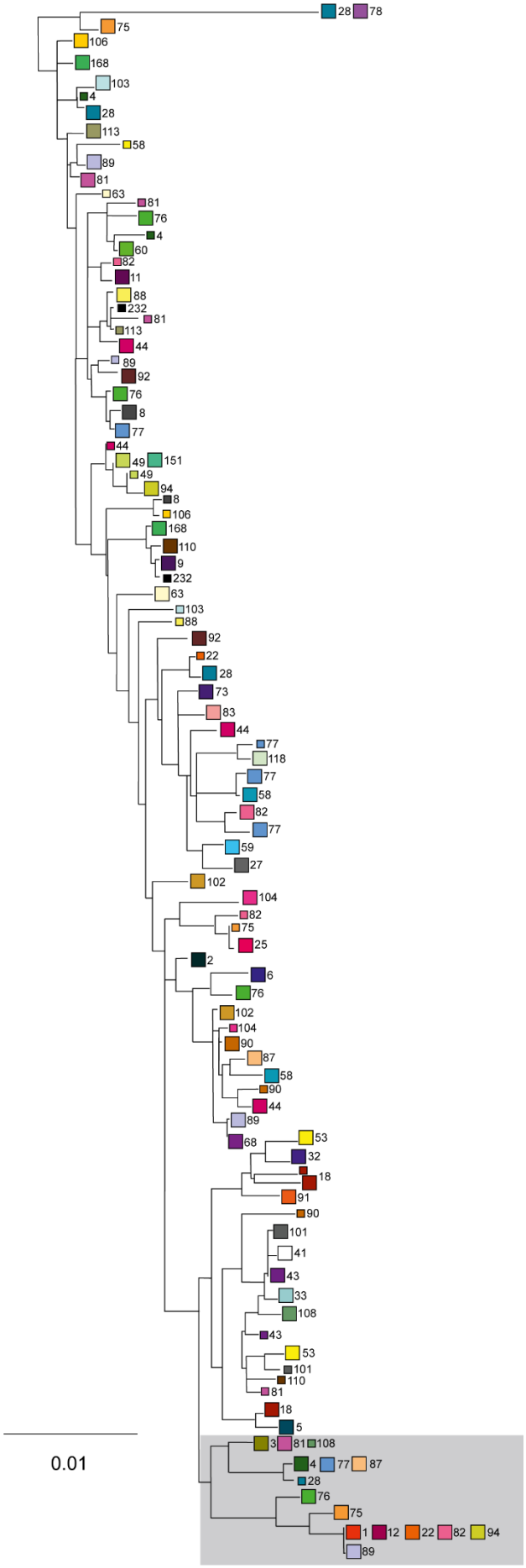

822

Figure 4. Variants of P-*nga*-*ifs*-*slo* within *emm* genotypes. The P-*nga*-*ifs*-*slo* was extracted from 5271 assembled genomes and aligned for SNP extraction, and these used for maximum likelihood midpoint-rooted phylogenetic tree construction. Squares represent multiple identical sequences (larger squares) or single sequences (smaller squares) of individual *emm*-types. The *emm*-type is given next to each square. Shaded region; high activity cluster. Scale represents substitutions per sites.

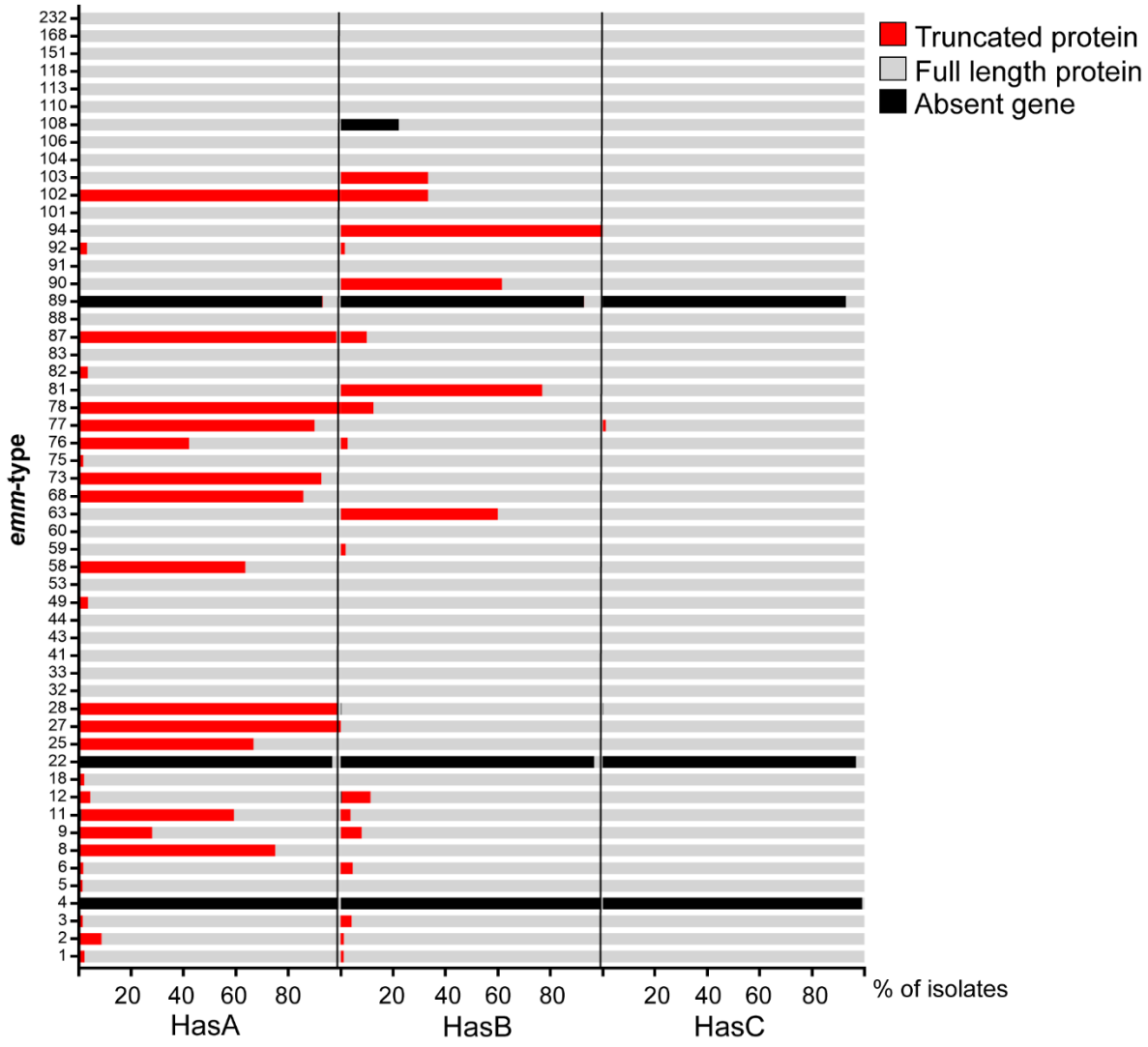

Figure 5. Non-functional mutations within the capsule locus genes. The *hasABC* genes were extracted from the assembled genomes of BSAC, CUH, PHE-2015/15, and ABCs-2015 isolate collections and polymorphisms or indels leading to nonsense mutations and premature stop codons were identified, as well as gene absence. The percentage of isolates with full length (grey), truncated (red) or absent (black) HasA, HasB or HasC is depicted for each of the 54 *emm*-types. *emm*-types with fewer than 3 isolates were excluded. N = 5271 isolates shown. Mutations in *hasA* were detected in more than 50% of isolates belonging to genotypes *emm*8 (n=3/4), *emm*11 (n=63/108), *emm*25 (n=2/3), *emm*27 (n=3/3), *emm*28 (n=358/363), *emm*58 (n=21/33), *emm*68 (n=12/14), *emm*73 (n=25/27), *emm*77 (n=72/80), *emm*78 (n=8/8), *emm*87 (n=119/121) and *emm*102 (n=6/6). Mutations in *hasB* were detected in 100% of

841 *emm*94 isolates (n=54/54) and 60-77% of *emm*63 (n=3/5), *emm*81 (n=50/65) and *emm*90

842 (n=16/26) isolates.

843

844

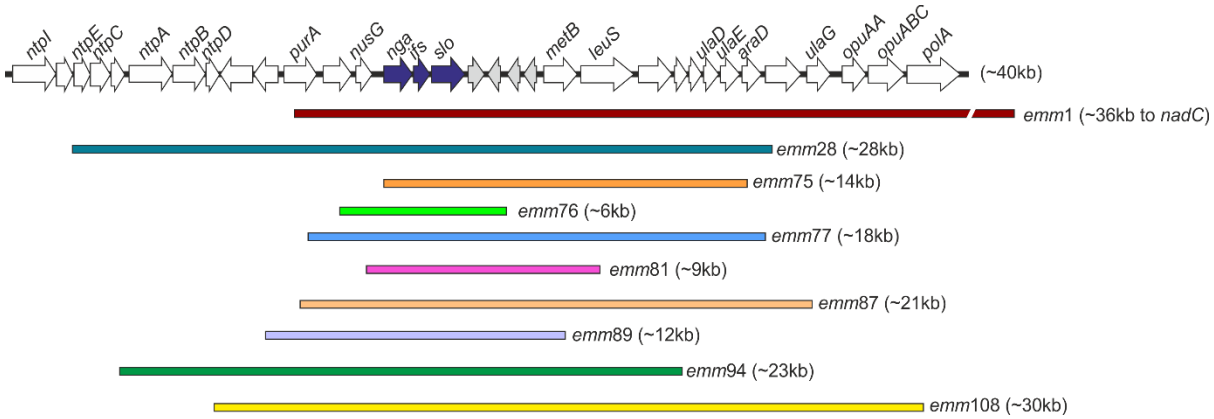

845

846

847 **Figure 6. Regions of recombination spanning the P-*nga-ifs-slo* locus.** Recombination
848 across the *nga*, *ifs* and *slo* genes (blue arrows) was identified in eight genotypes in addition to
849 the previously described *emm*1 and *emm*89. Length of recombination, predicted by SNP
850 cluster analysis, ranged from ~6kb to 36kb. With the exception of *emm*75, all regions also
851 encompassed the promoter of *nga-ifs-slo*. All regions are shown relative to a ~40kb region
852 within the reference genome H293 and genes within this region are depicted as arrows.
853 Recombination in *emm*1 extended beyond that depicted here and is shown as a broken line.

854

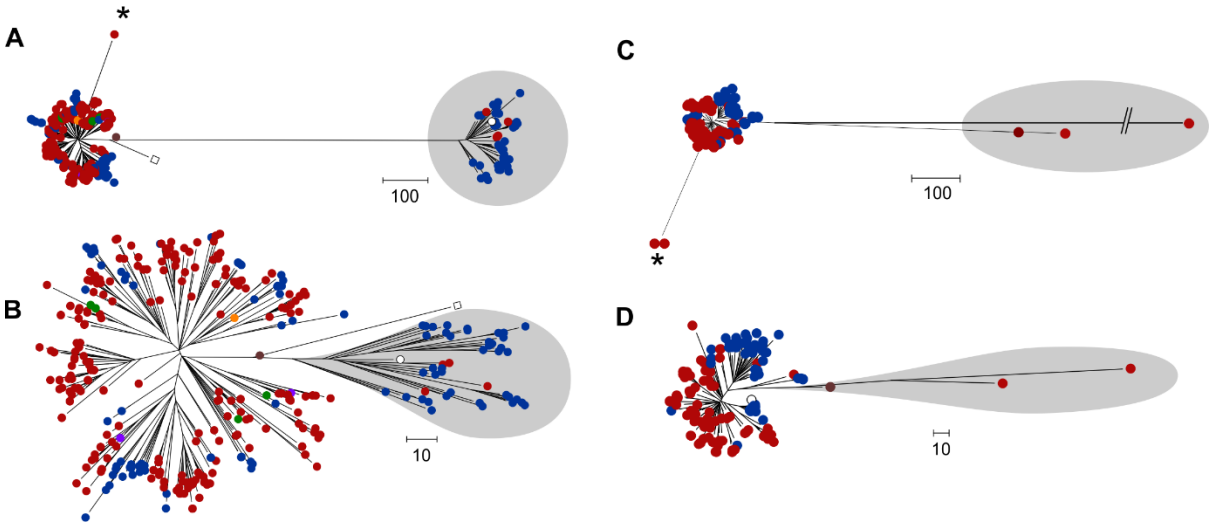

Figure 7. Recombination within the *emm*28 and *emm*87 populations. **(A)** Maximum likelihood phylogeny constructed with core SNPs following mapping of all available *emm*28 genome data to the *emm*28 MGAS6180 reference genome (white square) (18). Modern UK isolates (red circles); BSAC (n=15), CUH (n=13 (11)) and PHE-2014/15 (n=240 (12, 13)), one historical English isolate from 1938 (brown circle). North American isolates (blue circles); ABCs-2015 (n=95 (14)), Canada (2011-2013, n=4 (42)), and completed genome strain HarveyGAS (USA, 2017 (43)). Other isolates; Lebanon (n=1, orange circle (44)), Australia (n=5, green circle (45)), France (STAB10015 (46), M28PF1 (47), purple circles). Two lineages of *emm*28 were identified, one clustering with MGAS6180 (white square) and the other (shaded grey) clustering with MEW123 (2012 USA (19), white circle). (**B)** Regions of recombination were then identified within the *emm*28 genome alignment and removed before reconstructing the phylogenetic tree (**C**) Maximum likelihood phylogeny constructed with core SNPs following mapping of all available *emm*87 genome sequence data to the reference *emm*87 strain NGAS743 (Canada, white circle (48)). UK isolates (red circles); BSAC (2001-2011, n=22), CUH (2008, n=1 (11)), PHE-2014/15 (n=64, (12, 13)). North American isolates (blue circles); ABCs-2015 (n=26, (14)), Canada (n=26, (48)), Texas Children's Hospital (2012-2016, n=27, (49)). Three isolates (shaded grey) were distinct from

873 the main population. The branch was shortened for one isolate for presentation purposes. (**D**)
874 Regions of recombination were identified within the *emm*87 genome alignment and removed
875 before reconstructing the phylogenetic tree. Isolates indicated by * in both *emm*28 and
876 *emm*87 populations were predicted to have undergone recombination in regions surrounding
877 the *hasABC* locus. Scale bar represents single nucleotide polymorphisms. PHE-2014/15
878 *emm*28 isolates GASEMM1261, GASEMM2648, GASEMM1396 and GASEMM1353 were
879 removed for presentation purposes as they represented highly divergent lineages.

880

881

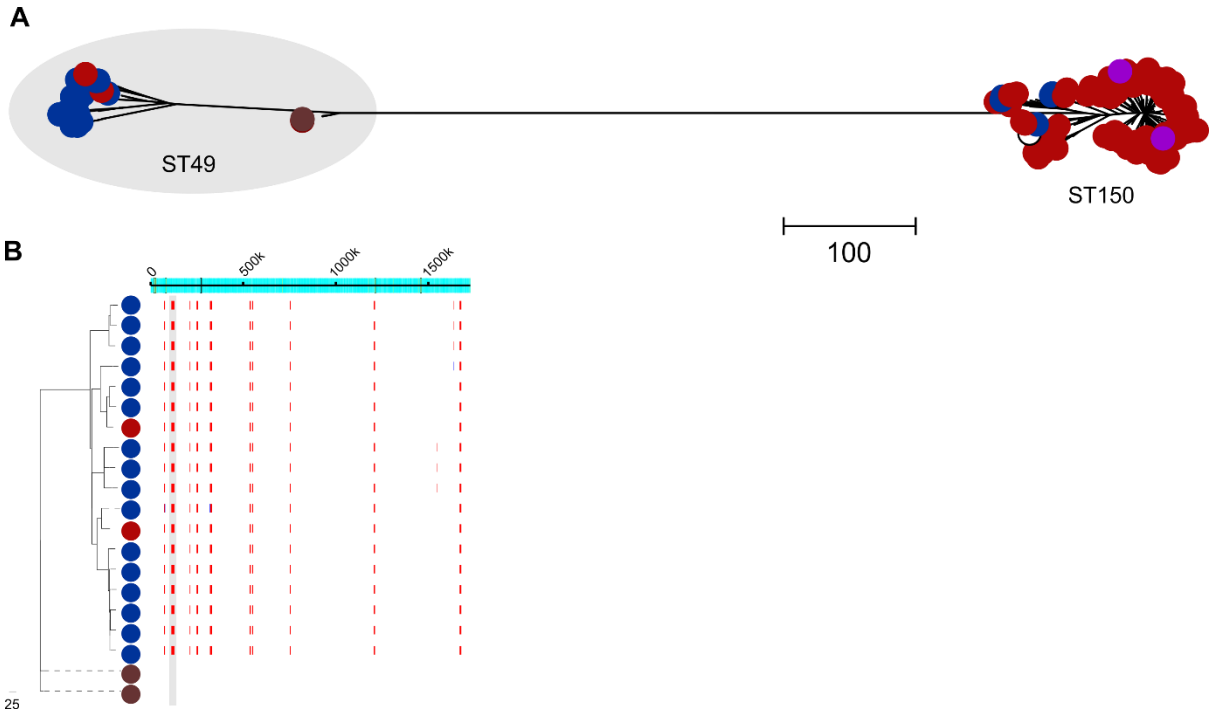

882

883 **Figure 8. Two lineages within *emm*75. (A)** Maximum likelihood phylogeny constructed
884 with core SNPs following mapping of all available *emm*75 genome sequence data to the
885 French strain STAB090229 (white circle) (50). Modern UK collections (red circles); BSAC
886 (n=11), CUH (n=6 (11)), PHE-2014/15 (n = 141, (12, 13)) and two English historical isolates
887 (brown circles) from 1937/1938. North American isolates (blue circles); ABCs-2015 (n=20,
888 (14)), NGAS344 and NGAS604 from Canada 2011/2012 (42). French strains (purple circles);
889 STAB120304 (2012) and STAB14018 (2014). Two lineages were identified, generally
890 characterised by the MLST; ST49 (shaded grey) or ST150 (with minor MSLT variants
891 ST788, ST851, ST861 within these lineages). (**B)** Gubbins analysis identified ten regions of
892 predicted recombination (red lines) in all modern ST49 compared to historical 1930s ST49
893 across the genome (indicated across the top). One region included P-*nga*-*ifs*-*slo* (shaded
894 grey). Scale bars represent single nucleotide polymorphisms. One PHE-2014/15 isolates
895 (GASEMM1722) was excluded for presentation purposes as it was highly divergent from the
896 rest of the population.

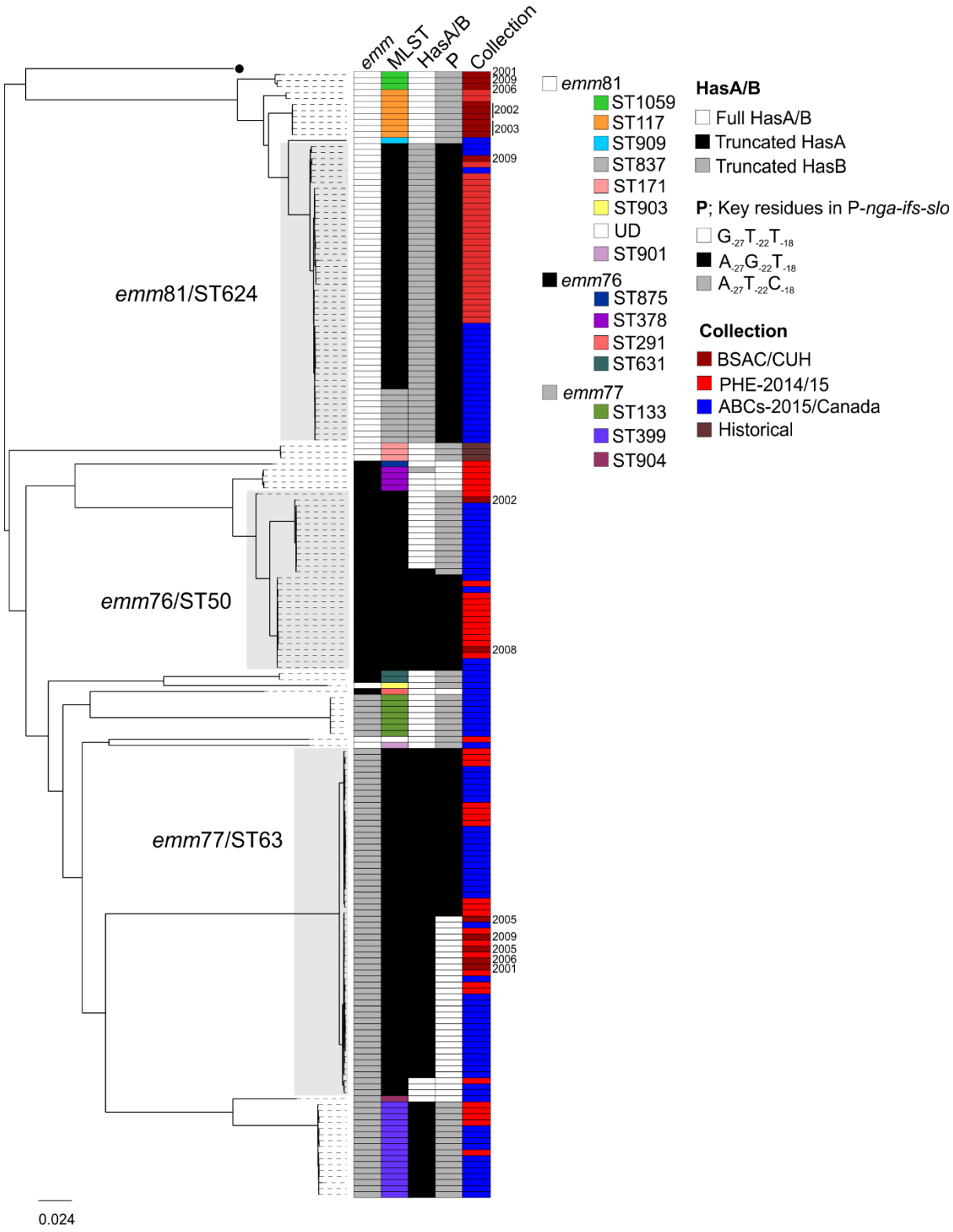

Figure 9. Variants of P-*nga-ifs-slo* and capsule mutations associated with lineages of *emm*76, *emm*77 and *emm*81. Maximum likelihood phylogeny identified multiple MLST lineages within the populations of *emm*76, *emm*77 and *emm*81 (STs provided in the key, UD;

901 undetermined). Major ST lineages are indicated and shaded grey. All *emm*81 isolates were
902 predicted to express full length HasA but the ST624, and minor (single base change in *recP*)
903 ST variant ST837, carry a mutation within *hasB* leading to a truncated HasB. For *emm*76 and
904 *emm*77, mutations were detected in *hasA*. We also identified variants of P-*nga-ifs-slo*
905 associated with one of three combinations of key promoter residues including the high
906 activity associated $A_{-27}G_{-22}T_{-18}$. Collection indicates either BSAC or CUH (dark red), PHE-
907 2014/15 isolates (red), North America (blue) or English historical (brown). Dates for BSAC
908 isolates and CUH are shown; other isolates were from 2014/2015 or 1930s (historical).
909 *emm*76; n=2 BSAC, n=18 PHE-2014/15 (12, 13), n=18 ABCs-2015 (14). *Emm*77; n=5
910 BSAC, n=21 PHE-2014/15 (12, 13), n=54 ABCs-2015 (14), n=2 Canada (date unknown)
911 (42). *emm*81; n=9 BSAC, n=1 CUH (11), n=29 PHE-2014/15 (12, 13), n=26 ABCs-2015
912 (14), n=3 historical 1930s. All sequence data was mapped to the reference strain H293 (black
913 circle). Scale bar represent substitutions per site.

914

915 **Supplementary Figures**

916

917

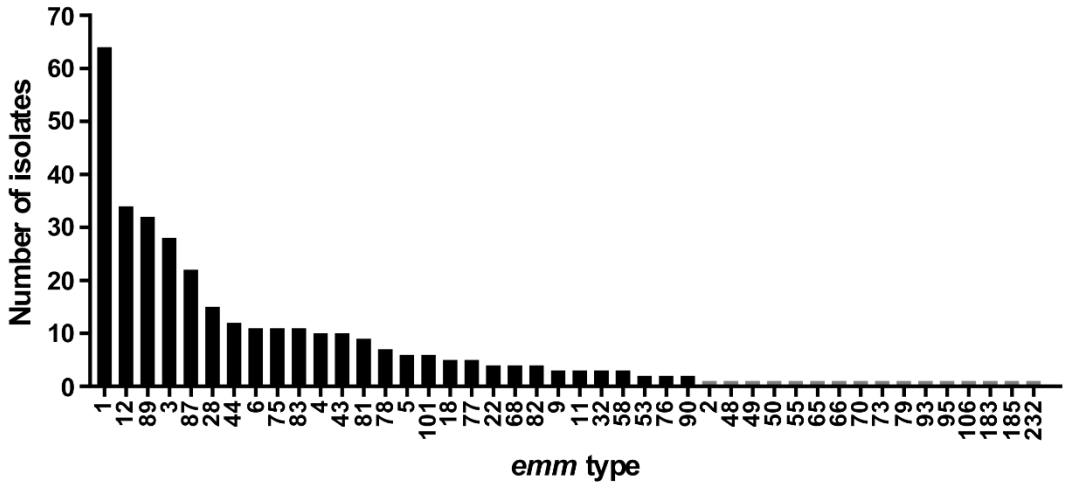

918

919 **Supplementary Figure 1.** Number of isolates per *emm*-type in the BSAC collection. Forty-

920 four different genotypes were identified within the collection but 16 were represented by

921 single isolates (grey bars). Total number of isolates was 344.

922

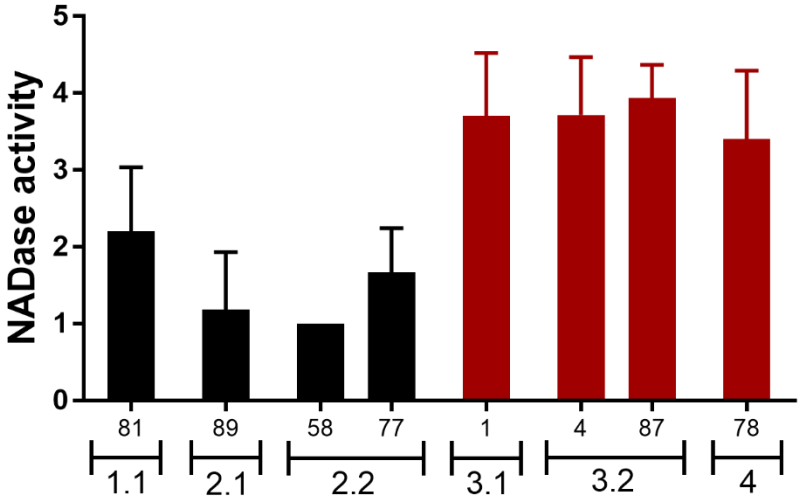

Supplementary Figure 2. NADase activity of different promoter subtypes. The activity of NADase was measured in culture supernatant of BSAC isolates representing different promoter subtypes with predicted low (black) or high (red) activity. $A_{-27}T_{-22}C_{-18}$ subtype 1.1 promoter has low activity in *emm*81 isolates, consistent with previous findings of this promoter in historical *emm*1. $G_{-27}T_{-22}T_{-18}$ subtype 2.1 had low activity in older *emm*89, also consistent with previous findings, and subtype 2.2 in *emm*58 and *emm*77 also had low activity, as predicted despite the additional base change at -40bp. High activity of $A_{-27}G_{-22}T_{-18}$ subtype 3.1 was confirmed in *emm*1 and subtype 3.2 in *emm*4 and *emm*87 also had high activity, also supporting a null effect of the base change at -40bp. $A_{-27}T_{-22}T_{-18}$ subtype 4 promoter in *emm*78 had high activity. Isolates with mutations in regulators *covR*/S or *rocA* were excluded as they influence the expression of *nga*. Data represent mean +SD of e*mm*1; n=10, *emm*89; n=11, *emm*58; n=3, *emm*77; n=3, *emm*4; n=7, *emm*87; n=17, *emm*78; n=5, *emm*81; n=5.

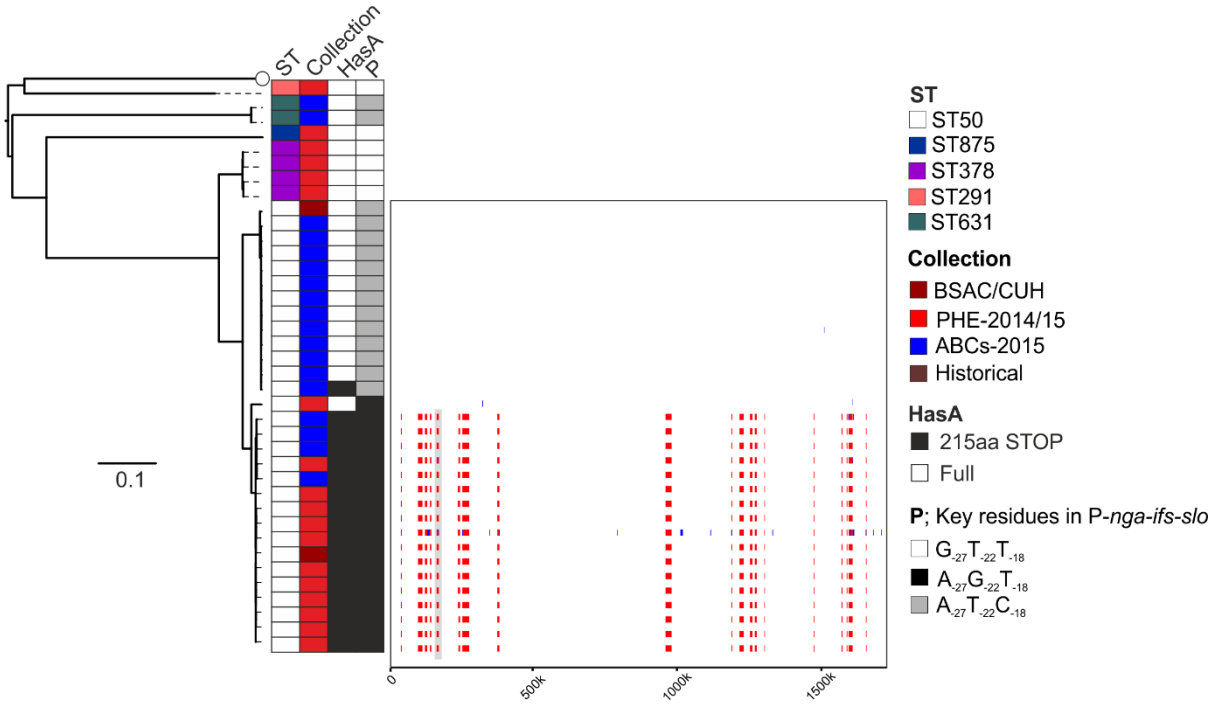

Supplementary Figure 3. Recombination within ST50 *emm*76. All sequence data for *emm*76 (n=38) were mapped to the reference strain H293 (white circle). Majority of isolates were ST50 and within this ST were two sub-lineages. Recombination analysis (boxed region) of ST50 isolates identified 19 regions of recombination across the genome in all isolates (red vertical lines) belonging to the lower sub-lineage compared to the top sub-lineage. One of these regions (highlighted grey) surrounded the P-*nfa*-*ifs*-*slo* locus conferring the high activity associated promoter with residues $A_{-27}G_{-22}T_{-18}$ to the lower sub-lineage compared to low activity $A_{-27}T_{-22}C_{-18}$ in the top sub-lineage. Scale bar represents substitutions per site. Scale on boxed region represents position in the H293 genome.

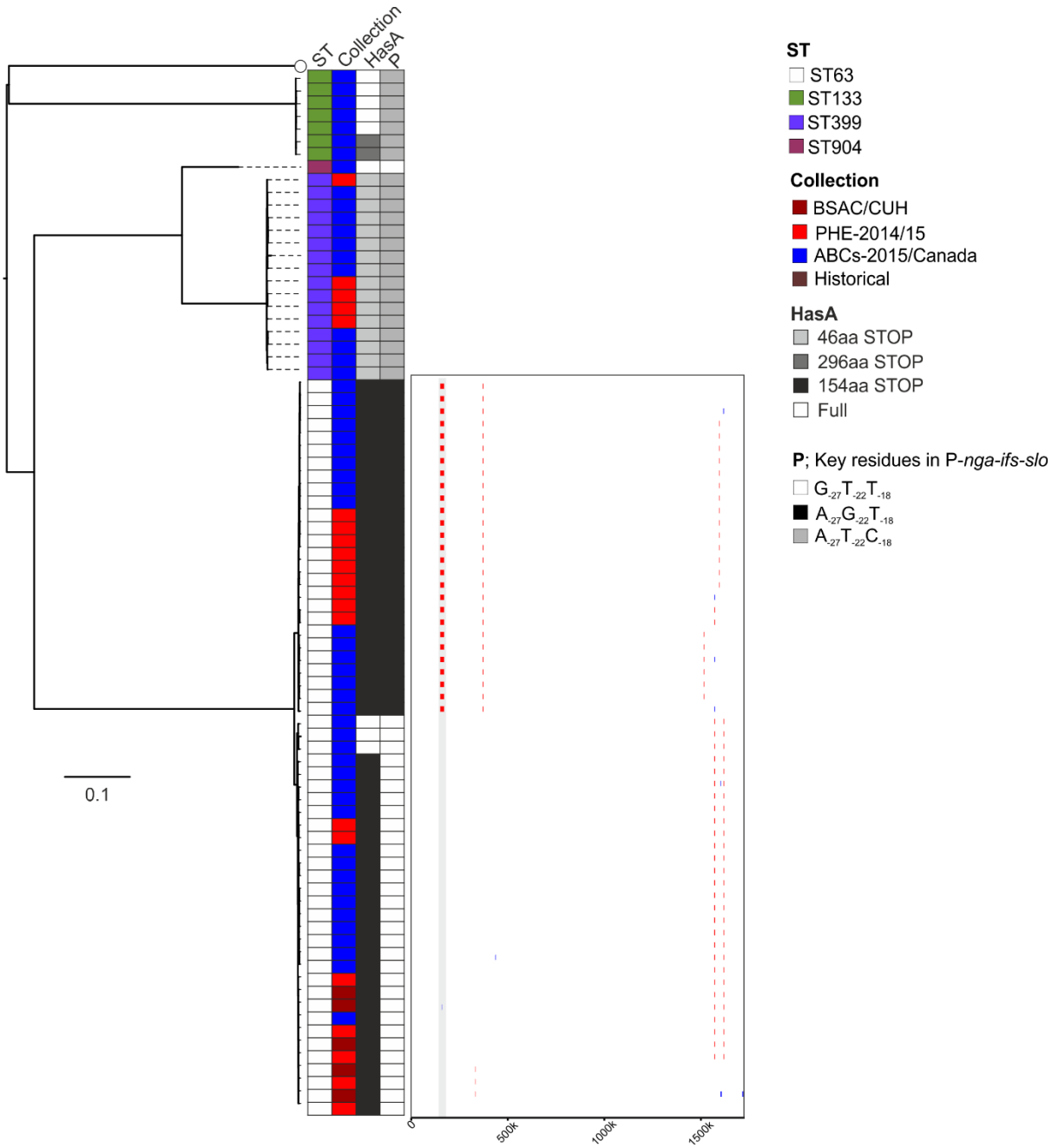

954

955

956 **Supplementary Figure 4. Recombination within ST63 *emm*77**. All sequence data for

957 *emm*77 (n=82) were mapped to the reference strain H293 (white circle). Majority of isolates

958 were ST63 and within this ST were two sub-lineages. Recombination analysis (boxed region)

959 of ST63 isolates identified 2 regions of recombination across the genome in all isolates (red

960 vertical lines) belonging to the top sub-lineage compared to the lower sub-lineage. One of

961 these regions (highlighted grey) surrounded the P-*nfa*-*ifs*-*slo* locus conferring the high

962 activity associated promoter with residues $A_{-27}G_{-22}T_{-18}$ to the lower sub-lineage compared to

963 low activity $G_{-27}T_{-22}T_{-18}$ in the top sub-lineage. Scale bar represents substitutions per site.

964 Scale on boxed region represents position in the H293 genome.

965

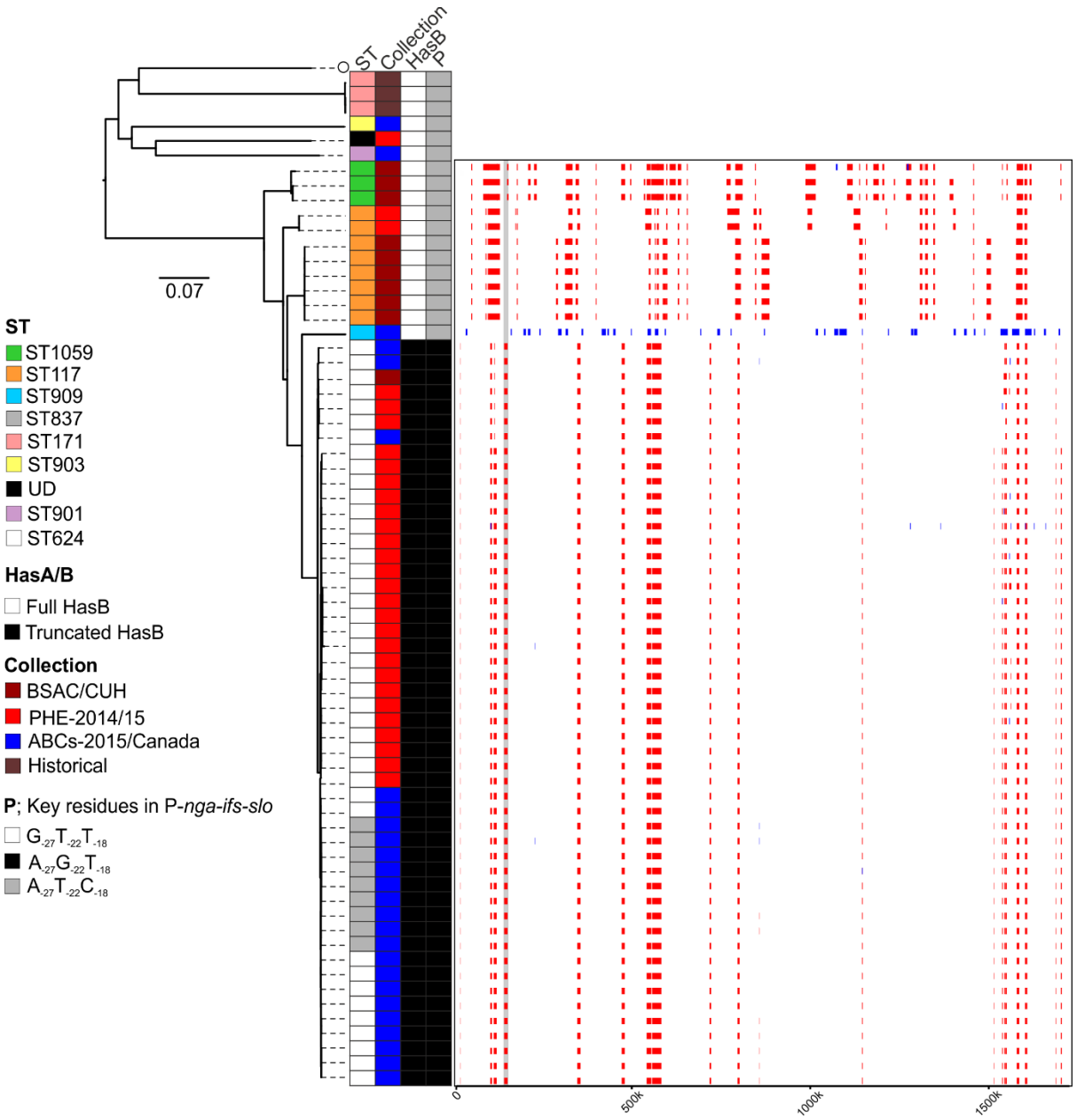

966

967

968 **Supplementary Figure 5. Recombination within *emm*81**. All sequence data for *emm*81

969 (n=68) were mapped to the reference strain H293 (white circle). Majority of isolates were

970 ST624. Recombination analysis (boxed region) of ST624 isolates and closely related ST1059,

971 ST117, ST909 and ST837 identified patterns of recombination across the genome in all

972 isolates (red vertical lines, or blue vertical lines if unique to a single isolate). One of these

973 regions (highlighted grey) surrounded the P-*nfa-ifs-slo* locus conferring the high activity

974 associated promoter with residues $A_{-27}G_{-22}T_{-18}$ to the ST624/ST837 population compared to

975 low activity $G_{-27}T_{-22}T_{-18}$ in all other isolates. Scale bar represents substitutions per site. Scale

976 on boxed region represents position in the H293 genome.

977

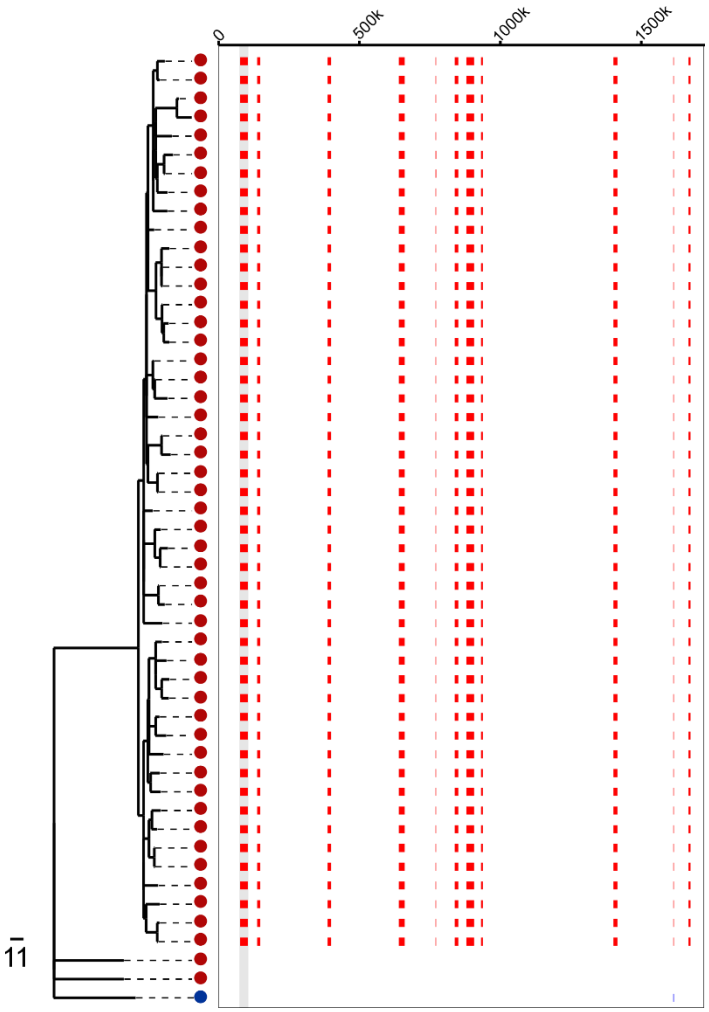

Supplementary Figure 6. Recombination in *emm*94. In the 2014/2015 UK *emm*94 population, the majority (n=51) form a lineage separate from two 2014/2015 UK isolates and the single 2015 USA isolate. SNP clustering analysis predicted 11 regions of recombination (red lines) in all the lineage associated isolates compared to the three other isolates. One of these regions (highlighted in grey) encompassed the P-*nga*-*ifs*-*slo* region. Scale bar represents SNPs.

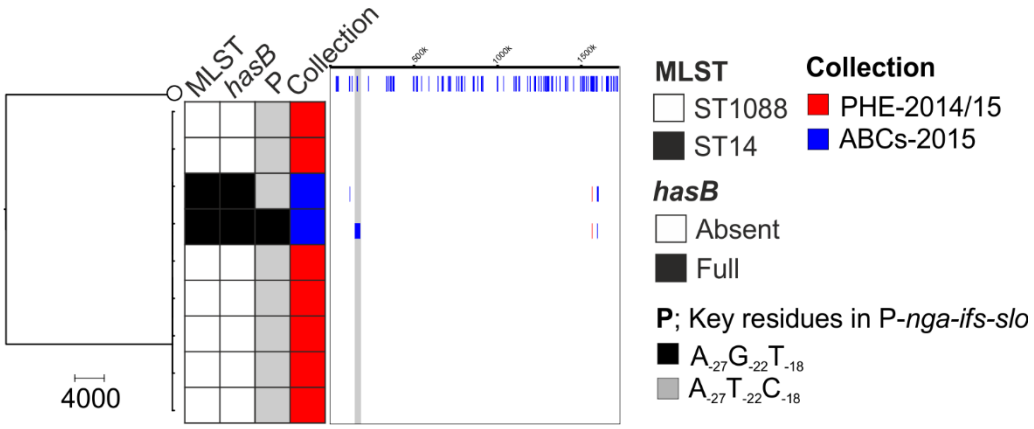

Supplementary Figure 7. Recombination in *emm*108 around P-*nga-ifs-slo*. Isolates of *emm*108 from the ABCs-2015 (blue) collection were of a different MLST (ST14) compared to PHE-2014/15 (ST1088). The *hasB* gene was absent in the genomes of both ABCs-2015 isolates and one had undergone recombination surrounding the P-*nga-ifs-slo* locus (shaded grey), as predicted by SNP cluster analysis (shown on the right). Blue lines; predicted recombination unique to a single genome. Sequence data were mapped to the reference strain H293, also used as an outgroup for SNP cluster analysis. Scale bar represents SNPs.

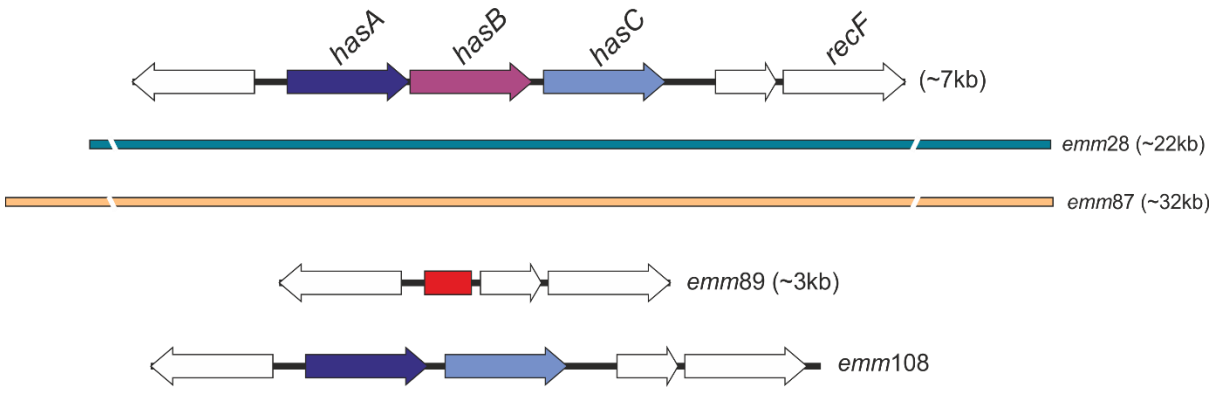

Supplementary Figure 8. Regions of recombination spanning the capsule locus.

Recombination across the *hasA, hasB* and *hasC* genes was identified in two genotypes in addition to the previously described *emm*89. Length of recombination, predicted by SNP cluster analysis, ranges from ~3kb to 32kb. Recombination within *emm*89 resulted in the loss of all three genes and the gain of a 150bp region (red). In *emm*108, the *hasB* gene was lost but this may be through recombination within the chromosome rather than recombination. All regions are shown relative to the reference genome H293 and genes within this region are depicted as arrows. Recombination in *emm*28 and *emm*87 extended beyond the region depicted and shown as broken lines.

Supplementary Tables

Supplementary Table 1 – Details of BSAC isolates and antimicrobial sensitivity testing

Excel File- Supplementary_Table_1.xlsx

Supplementary Table 2 – Details of all isolates with assembly statistics, capsule gene mutations and *nga/ifs/slo* promoter variants.

Excel File – Supplementary_Table_2.xlsx

Supplementary Table 3. Reference genomes used for mapping to in this study and excluded prophage regions

Reference strain	*emm* type	Prophage locations
H293	89	None
MGAS6180	28	986212-1032479
		1226909-1269223
		1807177-1821524
		1845845-1857621
		1081040-1092149
		1286346-1322672
STAB090229	75	723790-761364
		1138154-1180947
		1473588-1512859
NGAS743	87	547772-585345
		709624-756401
		1199244-1242181
		1253797-1293056